0012-9402/00/010033-19 $1.50 + 0.20/0
Birkhäuser Verlag, Basel, 2000

Eclogae geol. Helv. 93 (2000) 33–51

Climatic and environmental changes documented in the upper Paleocene to lower Eocene of Egypt

MARIE-PIERRE BOLLE[1], ABDEL AZIZ TANTAWY[2], ALFONSO PARDO[3], THIERRY ADATTE[1], STEVE BURNS[4] & AHMED KASSAB[5]

Key Words: Paleocene-Eocene transition, Egypt, climate, biostratigraphy, nannofossils, planktic foraminifera, stable isotopes, clay minerals

ABSTRACT

In a multidisciplinary approach including biostratigraphy, sedimentology, mineralogy and geochemistry, we attempt to reconstruct climatic evolution and environmental changes in Egypt from the late Paleocene to the early Eocene, with a special attention to the Late Paleocene Thermal Maximum (LPTM). In this region, despite the presence of short hiatuses at the planktic foraminiferal subzone P5a/b boundary, the LPTM interval is marked by a major turnover in the calcareous nannofossils coincident with the first appearance of the characteristic short ranging LPTM species *Acarinina sibaiyaensis*. This faunal turnover is accompanied by a negative $\delta^{13}C$ shift, a decrease of calcite and an increase of detrital quartz and high kaolinite contents. During the early Paleocene (Zone P3), this region experienced a warm and humid climate with high rainfall as indicated by the abundance of kaolinite in marine sediments. Subsequently, in Zones P4 and P5 seasonal climatic conditions with alternating wet and dry seasons evolved in this region as indicated by the low kaolinite content and the abundance of smectite. During the LPTM, southern Egypt was affected by a humid and warm climatic episode which persisted through the early Eocene (Zone P6). The presence of condensed phosphates coincident with high organic matter just above the LPTM is consistent with an upwelling activity at this time.

RESUME

Cette étude, basée sur une approche multidisciplinaire incluant biostratigraphie, sédimentologie, minéralogie et géochimie, a pour but la reconstitution climatique et environnementale en Egypte du Paléocène tardif à l'Eocène précoce, en accordant une attention spéciale au maximum thermique de la fin du Paléocène. En Egypte, malgré la présence de hiatus à la limite P5a/b, cet évènement est marqué par un renouvellement rapide de la faune de nannofossiles calcaires et par l'apparition d'une espèce de foraminifère planctonique (*Acarinina sibaiyaensis*). Ce renouvellement de faunes est associé à une chute de la sédimentation carbonatée, à une augmentation du détritisme et à un épisode à kaolinite. Au Paléocène précoce (Zone P3) cette région était marquée par un climat chaud et humide qui devenait saisonnier au Paléocène terminal (Zones P4 et P5). Durant le maximum thermique, cette région était affectée par un épisode climatique chaud et humide qui se prolongeait dans l'Eocène précoce (Zone P6). La présence de phosphates condensés et de sédiments riches en matière organique déposés après le maximum thermique suggèrent une activité de courants d'upwellings à cette période.

Introduction

The latest Paleocene is marked by major global climatic and environmental changes, which caused various paleontological, sedimentological, mineralogical and isotopic variations indicating an average warming of about 6°C in deep and high-latitude surface waters (referred to as the Late Paleocene Thermal Maximum or LPTM) (Kennett & Stott 1991; Zachos et al. 1993). In both high and low latitudes this warm pulse coincides with a pronounced short-term negative $\delta^{13}C$ excursion and the extinction of 35 to 50% of deep-sea benthic foraminiferal species (Thomas 1990; Kennett & Stott 1991).

The Tethys is a key region for investigating the potential cause(s) and mechanism(s) of the LPTM global changes. During the LPTM the Tethys was a semi-restricted basin surrounded by vast shallow epicontinental seas, undergoing intense tectonic activity (Oberhänsli & Hsü 1986; Klootwijk et al. 1992; Oberhänsli 1992; Selverstone & Gutzler 1993). These unique geographic and tectonic features suggest that the Tethys region was a major source of organic carbon (Raymo & Ruddiman 1992; Selverstone & Gutzler 1993) and warm saline deep water (Kennett & Stott 1990, 1991), two conditions that could have been the primary driving forces for the LPTM global climatic and environmental changes.

From the late Cretaceous to the Eocene, the southern margin of the Tethys was located in the northern tropical zone, affected by intermittent upwelling episodes. The long-term evo-

[1] Institut de Géologie, 11 Emile Argand, 2007 Neuchâtel, Switzerland, e-mail: marie-pierre.bolle@geol.unine.ch
[2] Geology Dpt., Aswan Faculty of Science, South Valley University, Egypt.
[3] Dpt. de Ciencas de la Tierra, Universidad de Zaragoza, 50009 Zaragoza, Spain.
[4] Geologisches Institut, Balzerstrasse, 3000 Bern, Switzerland.
[5] Geology Dpt., Assiut University, Egypt.

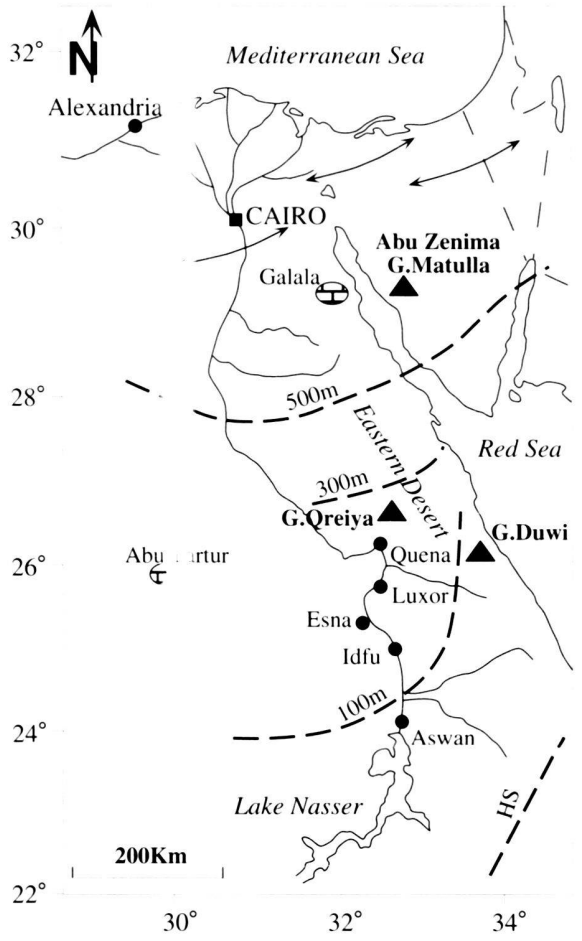

Fig. 1. Location of the studied profiles (black triangles) in Egypt. Palaeobathymetric reconstruction for the late Paleocene after Speijer & Van der Zwaan (1994). Areas with limestone symbols indicate carbonate platforms/ramps. Arrows indicate general direction of fold axes of the Sinai-Negev fold belt (a region of submarine and emerged land areas; Arkin et al. 1972; Said 1990). HS indicates hypothetical shore line (Speijer & Van der Zwaan 1994).

lution of this upwelling system is recorded in the widespread late Cretaceous to Eocene phosphate belt that extends from South America through North Africa as far as the Arabian Craton (Almogi-Labin et al. 1993). Recent detailed investigations of epicontinental Paleocene/Eocene sections located at the eastern end of this upwelling belt (Egypt and Israel) revealed similar major changes to those observed in coeval deep-sea sections; either a benthic foraminiferal extinction (Speijer 1994; Speijer & Van der Zwaan 1994; Speijer et al. 1996; Speijer & Schmitz 1998; Tantawy 1998; Speijer et al. in press), turnovers in planktic foraminifera (Lu et al. 1995) and calcareous nannofossils (Monechi et al. 1999; Tantawy 1998; Tantawy et al. 1999), and a negative $\delta^{13}C$ excursion (Charisi & Schmitz 1995, 1998; Lu et al. 1995; Schmitz et al. 1996). However, $\delta^{13}C$ values are significantly lower at the southern Tethyan margin than in other Tethyan and Pacific sections (Lu et al. 1995; Charisi & Schmitz 1995, 1998; Schmitz et al. 1996) reflecting regional effects probably caused by the restricted character of the southern Tethyan margin relative to the open ocean (Charisi & Schmitz 1998).

We attempt here to reconstruct the climatic evolution and environmental changes at the southern Tethyan margin, based on four sections reaching from middle neritic (Gebel Duwi, Eastern Desert) to upper bathyal depths (Gebel Matulla and Abu Zenima, Sinai; Speijer & Van der Zwaan 1994; Fig. 1). We present new biostratigraphic (nannofossil and planktic foraminifera), mineralogical (bulk rock and clay minerals) and total organic carbon content (TOC) data from the four Egyptian sections that span the late Paleocene to early Eocene. Stable isotope analyses provide additional stratigraphic control in locating the critical LPTM interval.

Localities, lithology and paleodepths

The Gebel Duwi section is located about 20 km to the west of the town of Quseir near the Red Sea coast of Egypt (26°06'N, 34°17'E). Benthic foraminiferal assemblages from this section suggest middle neritic conditions from the late Paleocene to early Eocene (75–100 m, Fig. 1; Speijer & Van der Zwaan 1994). The Gebel Qreiya section is located in the Eastern Desert to the NE of the town of Qena (26°21'N, 33°01'E). Speijer & Van der Zwaan (1994) estimate the paleodepth of the Gebel Qreiya section between 150–200 m (Fig. 1). The Gebel Matulla and Abu Zenima sections are located in the western Sinai (29°03'N, 33°10'E and 29° 03'N, 33°06'E respectively). Deposition occurred in an upper bathyal environment at about 500 m (Fig. 1; Speijer & Van der Zwaan 1994).

The part of the Gebel Duwi section studied here corresponds to the Esna Shale Formation (e.g. Said 1990). A total of 70 samples were collected from the Gebel Duwi section. This section consists mostly of marly shales becoming fissile in the upper 13 m. The most prominent feature is a 45 cm thick calcarenite bed overlying a 40 cm thick clayey interval (Fig. 2). The calcarenite contains shells, chalky mud pebbles, organic matter, abundant fish fossil remains and fecal pellets.

Thin sections of the calcarenite bed show irregular phosphatic pellets of various sizes (100 µm to 3 mm), phosphatized fish debris, abundant planktic foraminifera, very few detrital quartz grains and a non-phosphatized micritic matrix. The alternation of thin phosphate-poor layers containing few planktic foraminifera with phosphate-rich layers rich in planktic foraminifera suggest a condensed origin for the phosphatic sediment (K. Föllmi, pers. communication 1999).

The lowermost 1 m of the Gebel Qreiya section consists of shales attributed to the uppermost part of the Dakhla Formation (e.g. Said 1990). From 1 m to 6.1 m, the section is composed of marly limestones (Tarawan Formation; Said 1990) whereas the uppermost 7.9 m correspond to alternating marls and marly shales (lowermost part of Esna Formation, Fig. 2). No calcarenite bed has been observed in this section. A total of 66 samples were collected.

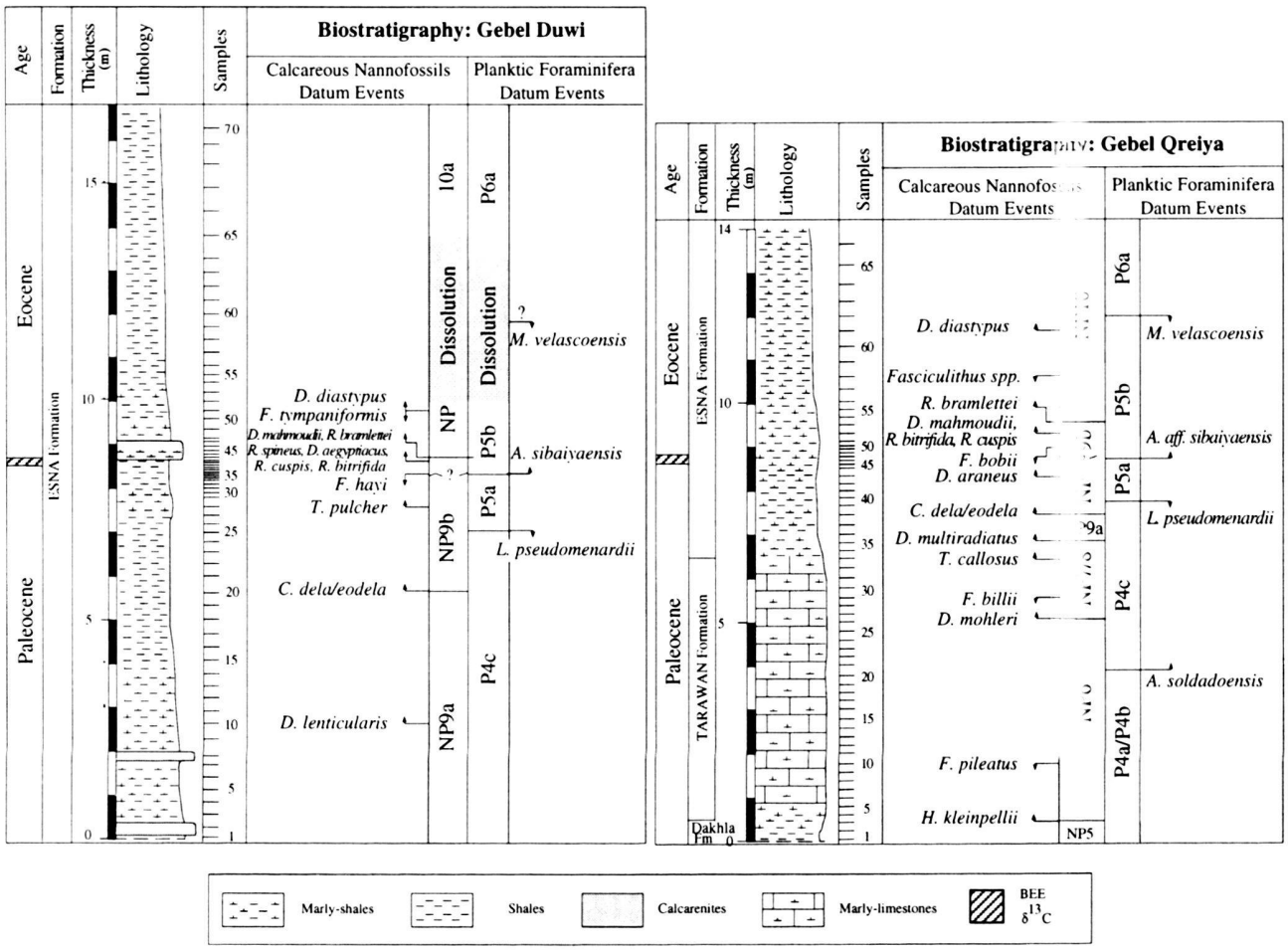

Fig. 2. Lithologic log with sample locations and biostratigraphic zonations of the Gebel Duwi and Gebel Qreiya sections, central Eastern Desert. LPTM = Late Paleocene Thermal Maximum interval.

The first 11 m of the Gebel Matulla section consist of 9 m of grey marly shales (corresponding to the Dakhla Formation in the Eastern and Western Desert) becoming marly limestones in the last 2 m (equivalent to Tarawan Formation). A bioturbated (*Thalassinoides*) hard ground (Hg, in Fig. 3) marks the top of this interval. Two thin calcarenite beds and one calcareous bed characterized the upper 12 m of the Esna Formation (Fig. 3). A total of 65 samples were collected.

The Abu Zenima section consists of marls which grade into shales upwards (Fig. 3). Towards the top of the section is a 10 cm thick calcarenite bed, followed by 30 cm of shales with burrows and a second calcarenite bed overlaid by marls containing fish fragments (Fig. 3). A total of 20 samples were collected at this section.

Methods

The biostratigraphy of the sections is based on planktic foraminifera (size fraction >106μm) and calcareous nannofossils. Calcareous nannofossils were analyzed from smear-slides using a light microscope and 1000x magnification. Oxygen and carbon stable isotopes analyses were based on the < 63μm size fraction of bulk rock samples. Analyses were conducted at the stable isotope laboratory of the University of Berne, Switzerland using a VG Prism II ratio mass spectrometer equipped with a common acid bath (H_3PO_4). The results were calibrated to the PDB scale with the standard errors of 0.1‰ for $\delta^{18}O$ and 0.05‰ for $\delta^{13}C$. X-Ray Diffraction (XRD) analyses of whole rock and clay minerals were conducted at the Geological Institute of the University of Neuchâtel, Switzerland using a SCINTAG XRD 2000 Diffractometer. Whole rock compositions were determined by XRD based on methods described by Ferrero (1966) and Kübler (1983). Clay mineral analyses followed the analytical method of Kübler (1987) described in Adatte et al. (1996), using the <2μm fraction here. Clay mineral fractions are given in relative abundance. Organic carbon was analyzed using a CHN Carlo-Erba Elemental Analyzer NA 1108 at the Geological Institute of the University of Neuchâtel.

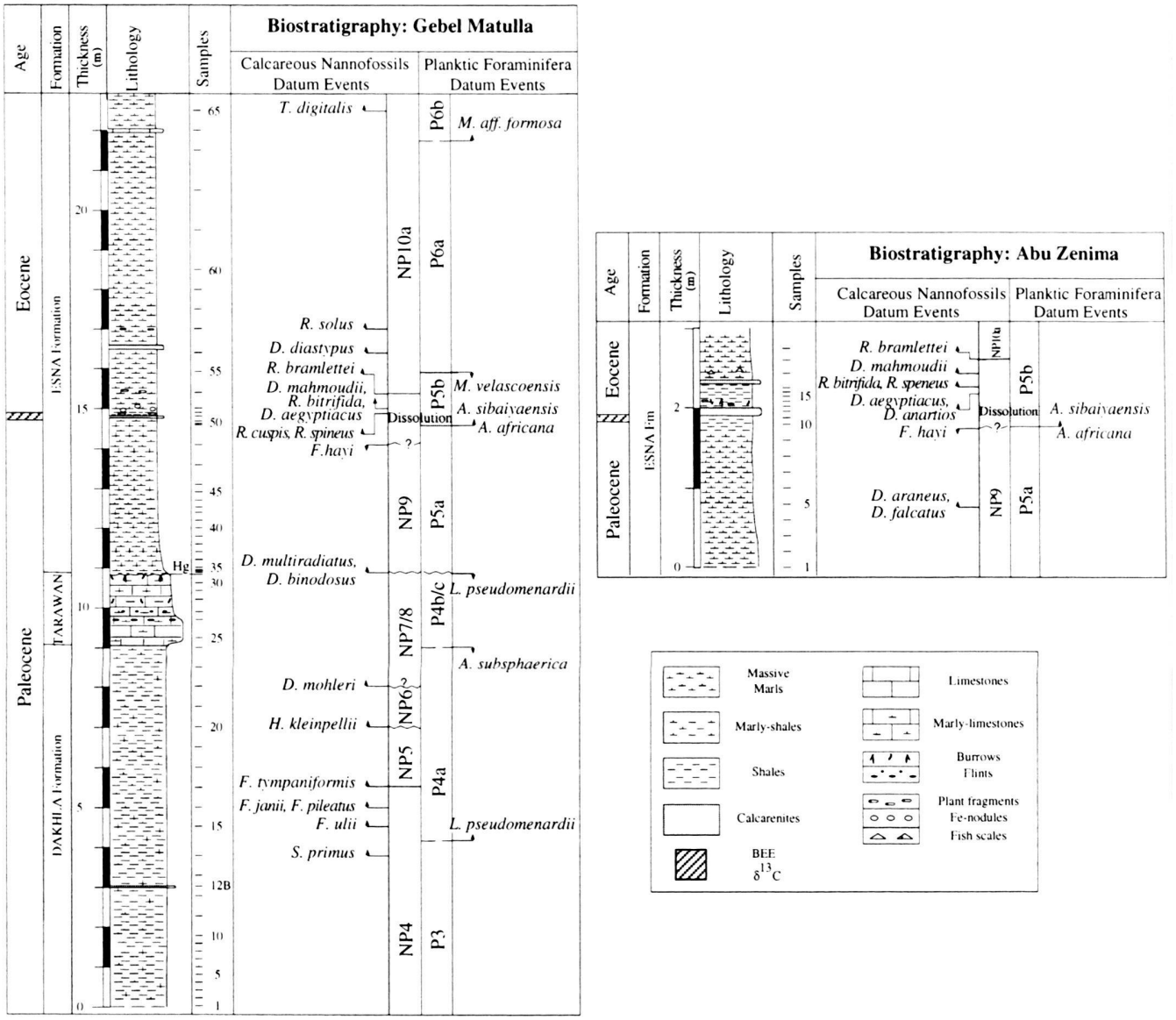

Fig. 3. Lithologic log with sample locations and biostratigraphic zonations of the Gebel Matulla and Abu Zenima sections, western Sinai.

Results

Biostratigraphy

Calcareous nannofossils

Calcareous nannofossils of the Egyptian Paleogene have been investigated by many workers over the last three decades (e.g. Tantawy 1998; Von Salis et al. 1998; Monechi et al. 1999). The current study concentrates on the late Paleocene-early Eocene (NP4 to NP9) biostratigraphy using the standard zonal scheme of Martini (1971), which is modified with respect to the definition of the combined NP7 and NP8 Zones by Romein (1979), and the subdivision of Zone NP9 into NP9a and NP9b (=CP8a and CP8b of Okada & Bukry 1980) (Figs. 2 and 3). In all sections, calcareous nannofossils are generally common to abundant, highly diverse and moderately to well preserved.

***Ellipsolithus macellus* Zone (NP4)**: Zone NP4 is present in the lower part of Gebel Matulla section (Fig. 3) where the top of this zone (FAD *F. tympaniformis*) is at 5.8 m. The base of NP4 was not recognized possibly due to dissolution or rarity of the index species *E. macellus*. This index species is also absent in the North Eastern Desert (Tantawy 1998). Its absence suggests dissolution effects and/or unfavorable environmental conditions (Monechi & Thierstein 1985; Wei & Wise 1989). Calcareous nannofossils assemblages of this zone are characterized by *Chiasmolithus danicus, Cruciplacolithus tenuis, C. edwardsii,*

C. primus, Neochiastozygus modestus, Prinsius tenuiculum and *P. bisulcus*. The first representatives of the *Fasciculithus (F. ulii, F. janii and F. pileatus)* and *Sphenolithus (S. primus)* lineages are observed in the upper part of this zone.

***Fasciculithus tympaniformis* Zone (NP5)**: In the Gebel Matulla section, strata from 5.8 m to 7.0 m are attributed to NP5 (Fig. 3). This interval contains a typical NP4 assemblage, but is distinguished by the presence of *Fasciculithus tympaniformis, Heliolithus cantabriae, Toweius pertusus, Bomolithus elegans* and *Neochiastozygus digitosus*. The top of this zone was also recognized at the base of the Qreiya section (Fig. 3).

***Heliolithus kleinpellii* Zone (NP6)**: At the Gebel Matulla section, NP6 is very short (Fig. 3) and may contain a hiatus. In contrast, at Gebel Qreiya this zone spans 4.5 m (Fig. 2). At both localities, the faunal assemblages of this interval are dominated by *C. tenuis, Coccolithus pelagicus, Ericsonia cave/ovalis, F. tympaniformis, F. janii, F. billii, F. bobii, H. cantabriae, H. kleinpellii, N. digitosus, T. pertusus, T. eminens, Sullivania consueta* and *Sphenolithus primus*.

***Discoaster mohleri* Zone (NP7/8)**: Because the species *Heliolithus riedelii* is rare or difficult to identify, the *D. mohleri* Zone was established by Romein (1979) to mark the interval spanning the *D. mohleri* and *H. riedelii* zones of Bramlette & Sullivan (1961). Zone NP7/8 is represented at Gebel Matulla and at Gebel Qreiya (Figs. 2 and 3). The assemblages in this interval are characterized by *D. mohleri, F. tympaniformis, F. clinatus, C. tenuis, S. consueta, Zygodiscus sigmoides, E. cava/ovalis, C. pelagicus, H. kleinpellii, H. cantabriae, S. primus, T. pertusus* and *D. nobilis*. *Fasciculithus billii* last occurs in the lower part of this zone, while *Toweius callosus* first appears in the upper part.

***Discoaster multiradiatus* Zone (NP9)**: Zone NP9 includes the interval from the first appearance datum (FAD) of *D. multiradiatus* to the FAD of *Rhomboaster (Tribrachiatus) bramlettei*. The FAD of *Campylosphaera dela/eodela* lies high up in Zone NP9 of both the Gebel Duwi and Qreiya sections. This agrees well with the occurrence reported by Okada & Bukry (1980), Perch-Nielsen (1985) and Bybell & Self-Trail (1997). Hence, the FADs of *Campylosphaera dela/eodela* appear to be synchronous and good markers for subdividing NP9 into subzones a and b, as proposed here for the central Eastern Desert sections. However, *C. dela/eodela* is very rare in both Gebel Matulla and Abu Zenima sections so that this subdivision cannot be applied in the Sinai.

Most *Fasciculithus* species, such as *F. hayi, F. clinatus, F. lillianae, F. bobii, F. alanii* and *F. mitreus* disappear near the top of NP9; other species which disappear include *H. cantabriae, H. kleinpellii, C. tenuis* and *E. macellus*. Species which first appear include: *C. dela/eodela, Fasciculithus thomasii, Transversopontis pulcher, Lophodolithus nascens* as well as many *Discoaster* species like *D. lenticularis, D. binodosus, D. araneus, D. mahmoudii, D. aegyptiacus* and *D. anartios*. In addition, the first representatives of the genus *Rhomboaster (R. cuspis, R. spineus* and *R. bitrifida*) appear in the uppermost part of NP9.

The base of NP9 is just at the top of the Tarawan Formation in the studied sections, though the Tarawan Fm. was not sampled at Abu Zenima and Gebel Duwi (Figs. 2 and 3). At the Gebel Matulla section an erosion surface and hardground marks the top of the limestone and a short hiatus (lower part of NP9 missing) is present between Zones NP7/8 and NP9 as suggested by the FAD's of *D. binodosus* and *D. multiradiatus*.

A dissolution zone (~10 cm thick) is observed in the upper part of NP9 in the Sinai sections (Gebel Matulla, samples 50 to 51; and Abu Zenima, samples 11 to 13). This dissolution interval has resulted in a notable decrease, or absence of calcareous nannofossils species, within a reddish to yellow 10 cm thick calcarenite horizon. Similar dissolution intervals have been recorded from the upper part of Zone NP9 in many localities, including DSDP Sites 549 and 550 (Aubry et al. 1996), Caravaca in Spain (Angori & Monechi 1996), Sites 525 and 527 (Thomas & Shackleton 1996), and the Clayton and Island Beach boreholes in New Jersey (Bybell & Self-Trail 1997).

***Tribrachiatus contortus* Zone (NP10)**: This zone spans the interval from the FAD of *Rhomboaster (T.) bramlettei* to the last appearance datum (LAD) of *T. contortus*. Only the lower part of this zone (NP10a Subzone of Aubry 1996) was sampled in the Egyptian sections (Figs. 2 and 3). At the Gebel Duwi section, carbonate dissolution marks a 3 m thick interval largely devoid of calcareous nannofossils near the base of NP10 (Fig. 2).

The LAD of *Fasciculithus* spp. has been used by many authors to approximate the NP9/NP10 boundary. In the Egyptian sections, the diversity and abundance of representatives of the genus *Fasciculithus* decreases notably and the genus disappears in the lower part of Zone NP10; the last occurrences of *Fasciculithus* species (*F. tympaniformis, F. involutus* and *F. thomasii*) are observed 1 m above the FAD of *R.(T.) bramlettei* at both Gebel Qreiya and Gebel Duwi sections (Fig. 2). In contrast, *F. tympaniformis* very rarely extends through the sampled NP10 intervals at Gebel Matulla and Abu Zenima sections. Thus, based on the Egyptian sections, the FAD of R. *(T.) bramlettei* is a more reliable zonal marker for the base of NP10. An additional marker event is the change in relative abundance of *Prinsiaceae* to *Coccolithus pelagicus*, where the former is more abundant in NP9 and the latter in NP10 (Von Salis et al. 1998; Tantawy et al. 1999). Thus, the „*C. pelagicus* acme" can be used to recognize the LPTM interval in sections where other markers are rare or absent.

In recent papers there has been an as of yet unresolved controversy about the correct determination and generic assignment – *Rhomboaster* or *Tribrachiatus*- of this species (e.g. Romein 1979; Perch-Nielsen 1985; Bybell & Self-Trail 1995, 1997; Angori & Monechi 1996; Aubry 1996; Wei & Zhong 1996; Aubry & Requirand 1999; Von Salis et al. 1999). Here we use *R.(T.) bramlettei* which is clearly distinguished from *R. cuspis, R. bitrifida* and *R. spineus* and placed the NP9/NP10 zonal boundary at the FAD of *R. (T.) bramlettei* following the original definition of Martini (1971).

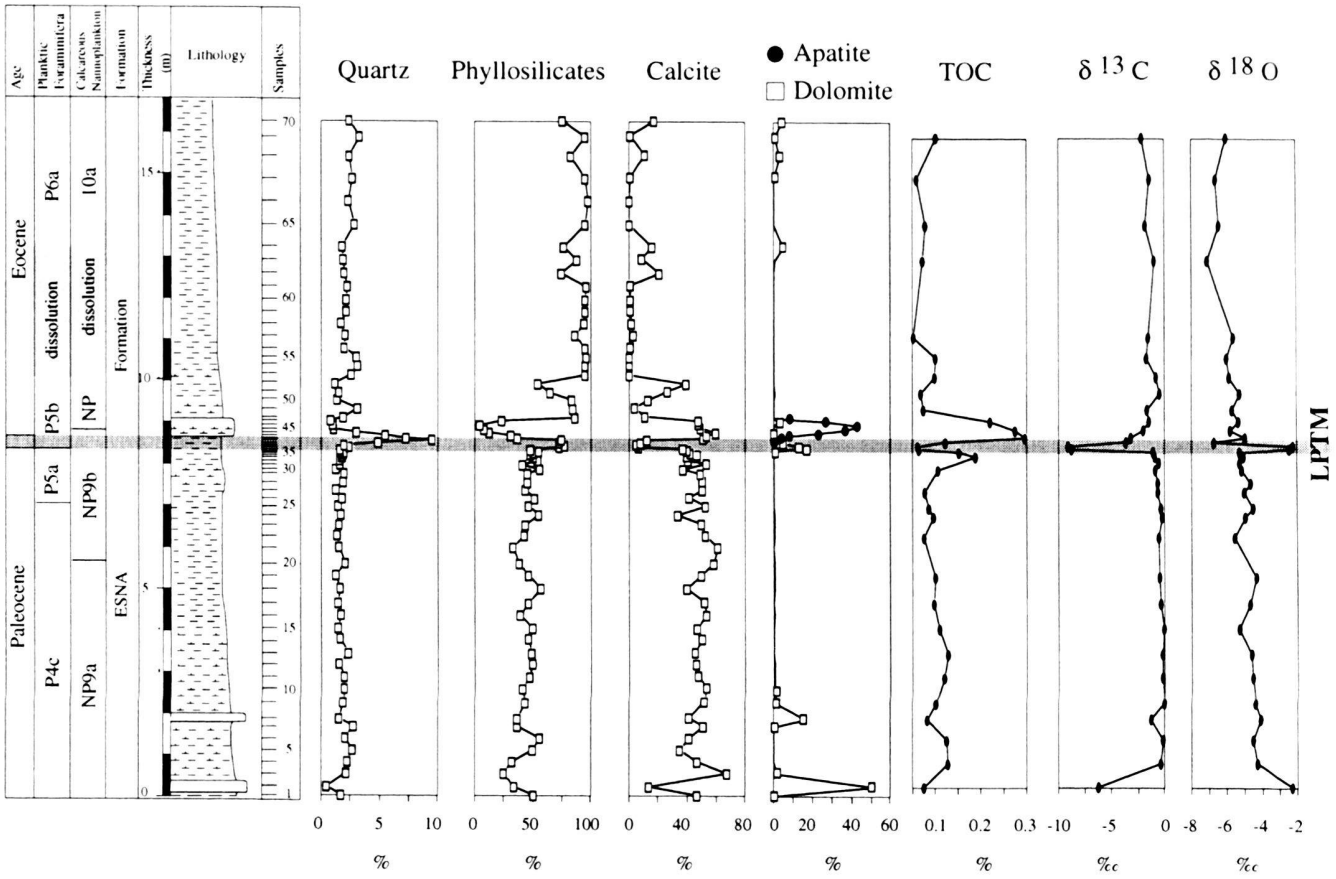

Fig. 4. Bulk rock mineral compositions, total organic content (TOC) and stable isotopic trends at Gebel Duwi. Stable isotopes analyses were conducted on the fine fraction (< 63 µm) of the bulk samples. See Fig. 2 for symbol explanation.

Planktic foraminifera

The planktic foraminiferal biostratigraphy of the four sections is based on the revised zonation by Berggren et al. (1995) and the subdivision of Zone P5 into Subzones P5a and P5b by Pardo et al. (1999a). Preservation of tests is poor to very good, surface textures and most morphological features are easily identifiable, though tests are commonly recrystallized.

Zone P3: Among the four sections studied for this report, only Gebel Matulla ranges down P3. In this outcrop Zone P3 spans approximately 4 m (Fig. 3).

Zone P4: In the Gebel Duwi section, the lowermost 7 m correspond to Subzone P4c. *Muricoglobigerina soldadoensis*, the index species for Subzone P4c, is present in the entire interval. Subzone P4b is defined as the interval between the LAD of *Acarinina subsphaerica* and the FAD of *Acarinina soldadoensis*. At Gebel Qreiya, no *A. subsphaerica* specimens where observed in the lower 4 m, suggesting that the entire interval corresponds to Subzone P4b. In this section, Subzone P4c reaches from 4 m to 7.6 m (Fig. 2). At Gebel Matulla, Zone P4 spans approximately 7 m; the first 4.5 m belong to Subzone P4a and the upper 2.5 m to Subzones P4b/c, where the LAD of *L. pseudomenardii* occurs (Fig. 3). In these three intervals, Zone P4 is characterized by morozovellids like *Morozovella velascoensis*, *M. aequa*; abundant subbotinids (*Subbotina velascoensis* and *S. eocaenica*), acarininids (*Acarinina acarinata*, *A. wilcoxensis*) but rare chiloguembelinids and muricoglobigerinids.

Zone P5: Pardo et al. (1999a) subdivided Zone P5 into two subzones based on the FAD of *A. sibaiyaensis* and/or *A. africana*. The FADs of these two short-ranging acarininid taxa coincide in the Tethyan realm (Lu et al. 1996, 1998; Pardo & Keller 1996; Pardo et al. 1999b) and Pacific Ocean (Kelly et al. 1995; Bralower et al. 1995) with the benthic foraminiferal extinction event (BEE), the negative carbon isotopic shift and the planktic foraminiferal diversification which characterize the LPTM.

Characteristic planktic foraminiferal species of Zone P5 in-

Gebel Qreiya

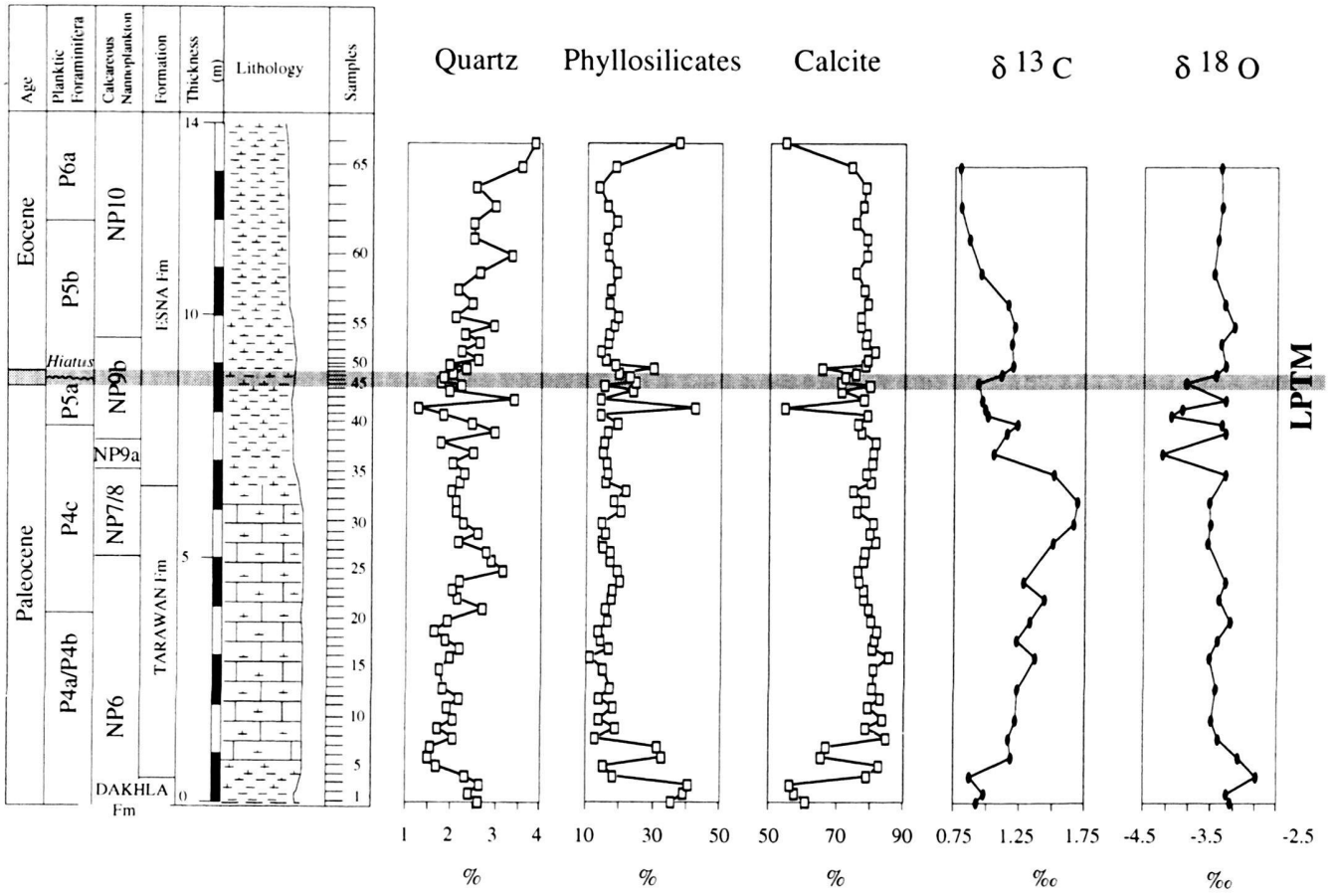

Fig. 5. Bulk rock mineral compositions and stable isotopic trends at Gebel Qreiya. Stable isotopes analyses were conducted on the fine fraction (< 63 μm) of the bulk samples. See Fig. 2 for symbol explanation.

clude *Morozovella velascoensis*, *M. subbotinae*, *M. aequa*; *Subbotina velascoensis*, *S. eocaenica*; *Acarinina acarinata*, *A. sibaiyaensis*, *A. berggreni*, *A. strabocella*; *Igorina pusilla* and *Globanomalina luxorensis*.

At Gebel Duwi, Subzone P5a spans ~1.4 m (Fig. 2). The top of P5a is not marked by the sudden appearance of abundant *A. sibaiyaensis*, which is not very common in this interval and no *A. africana* have been recorded, suggesting the possibility of a small hiatus at the P5a/P5b boundary (Fig. 2). A hiatus is also suggested by the unusually brief $\delta^{13}C$ excursion (Fig. 4). At Gebel Qreiya, Subzone P5a spans ~1 m, again the top of P5a is not clearly defined, since only very rare *A. sibaiyaensis* have been recorded, suggesting the presence of a hiatus that obliterated the *A. sibaiyaensis* and *A. africana* interval (Fig. 2). At Abu Zenima P5a spans ~2 m whereas at Gebel Matulla P5a spans approximately 4.5 m, from samples 31 to 51 where the first low ranging acarininids first appear (Fig. 3).

At Gebel Qreiya, Subzone P5b spans ~ 3.2 m whereas at Gebel Duwi, the top of Subzone P5b can not be identified due to the presence of a dissolution interval from 10 m up to 13 m (Fig. 2), where all foraminiferal tests are completely dissolved. At Abu Zenima P5b spans ~1 m up to the top of the studied section. Both index taxa, *A. sibaiyaensis* and *A. africana*, are common, suggesting a relatively complete sedimentary succession. At Gebel Matulla this subzone spans approximately 1.5 m, and shows the typical increase of warm water taxa, suggesting a relatively complete succession.

Zone P6: Of the two Subzones P6a and P6b, only P6a is present in the studied sections, characterized by species, such as *Morozovella subbotinae*, *M. gracilis*, *M. margiodentata*; *Acarinina acarinata*, *A. strabocella*, *A. quetra*; *Pseudohastigerina wilcoxensis* and *Luterbacheria elongata*.

Subzone P6a corresponds to the uppermost 2 m of the Gebel Qreiya section and to the uppermost 2 m of the Gebel Duwi section. At Gebel Matulla Subzone P6a spans at least 6 m. In sample 63 some transitional specimens to the morphotype *M. formosa* were recorded indicating the proximity of P6b (Fig. 3).

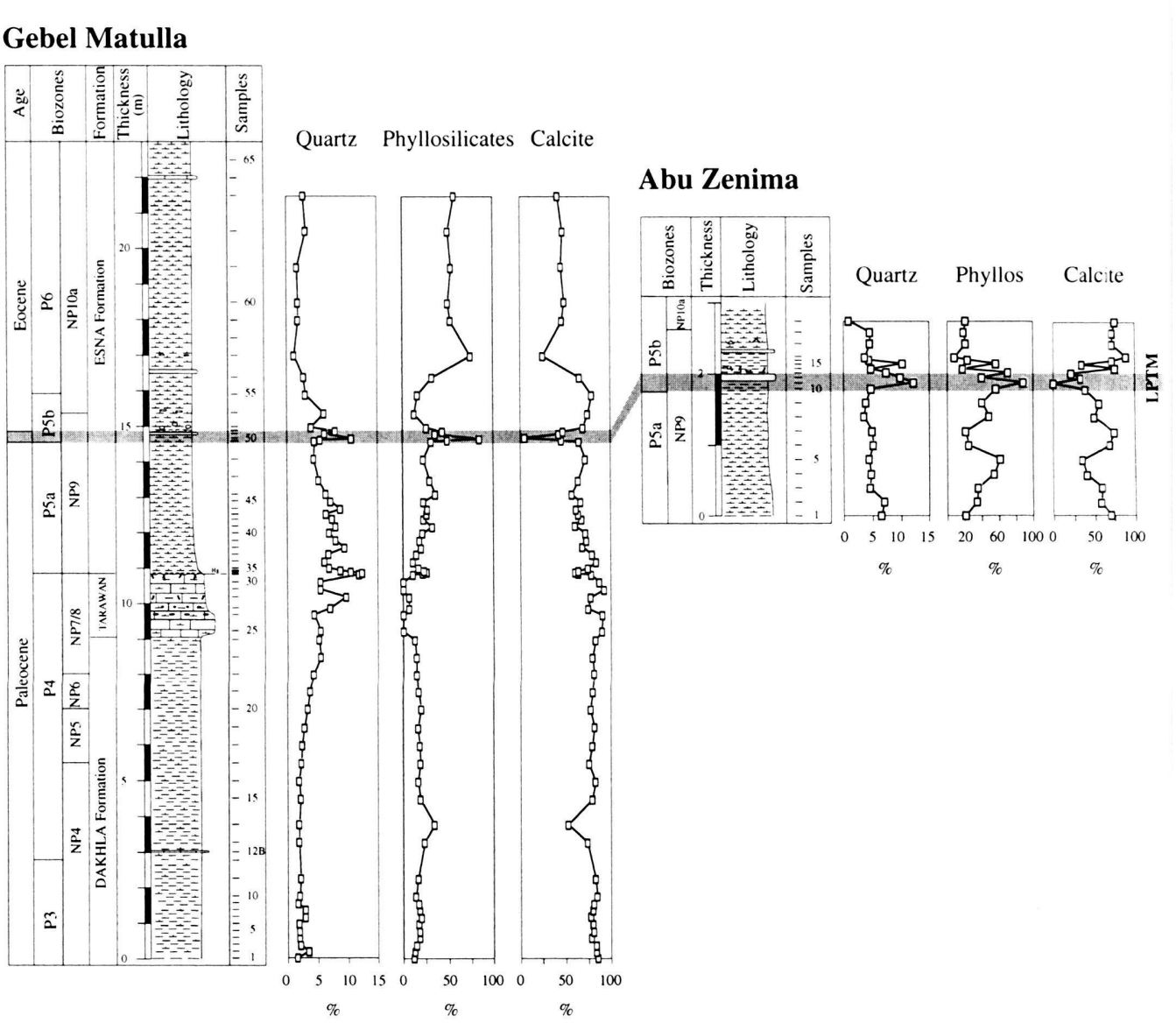

Fig. 6. Bulk rock mineral compositions at Gebel Matulla and Abu Zenima. See Fig. 3 for symbol explanation.

Mineralogy

Bulk rock

Bulk rock compositions were analyzed in the marine sediments of the four Egyptian sections in order to evaluate changes in sediment sources, proximity of terrigenous source areas and intensity of erosion and transport associated with potential sea level changes.

Gebel Duwi: Bulk rock composition of this section is highly variable (Fig. 4). In the lower part (from the base to 8.3 m) calcite (47%), phyllosilicates (46%) and quartz contents are relatively constant. The LPTM interval is 20 cm thick (samples 38 to 41) and marked by an abrupt decrease in calcite to 5%, coinciding with an increase in phyllosilicates to 74% and in quartz.

The calcarenite bed above the LPTM interval marks a calcite content recovery to 50% and a restricted occurrence of apatite, with a maximum value of 44%. Above the calcarenite bed, from 9.1 m to the top of the section, calcite contents fluctuate between 40% and 0%. The minimum corresponds to an interval of dissolution (samples 52 to 62) (Fig. 4). Dolomite is restricted to the two calcarenite beds (52% and 17%) in the lower part of the section and to the base of the LPTM interval (15%) (Fig. 4). Anhydrite and halite are minor components of the sediment.

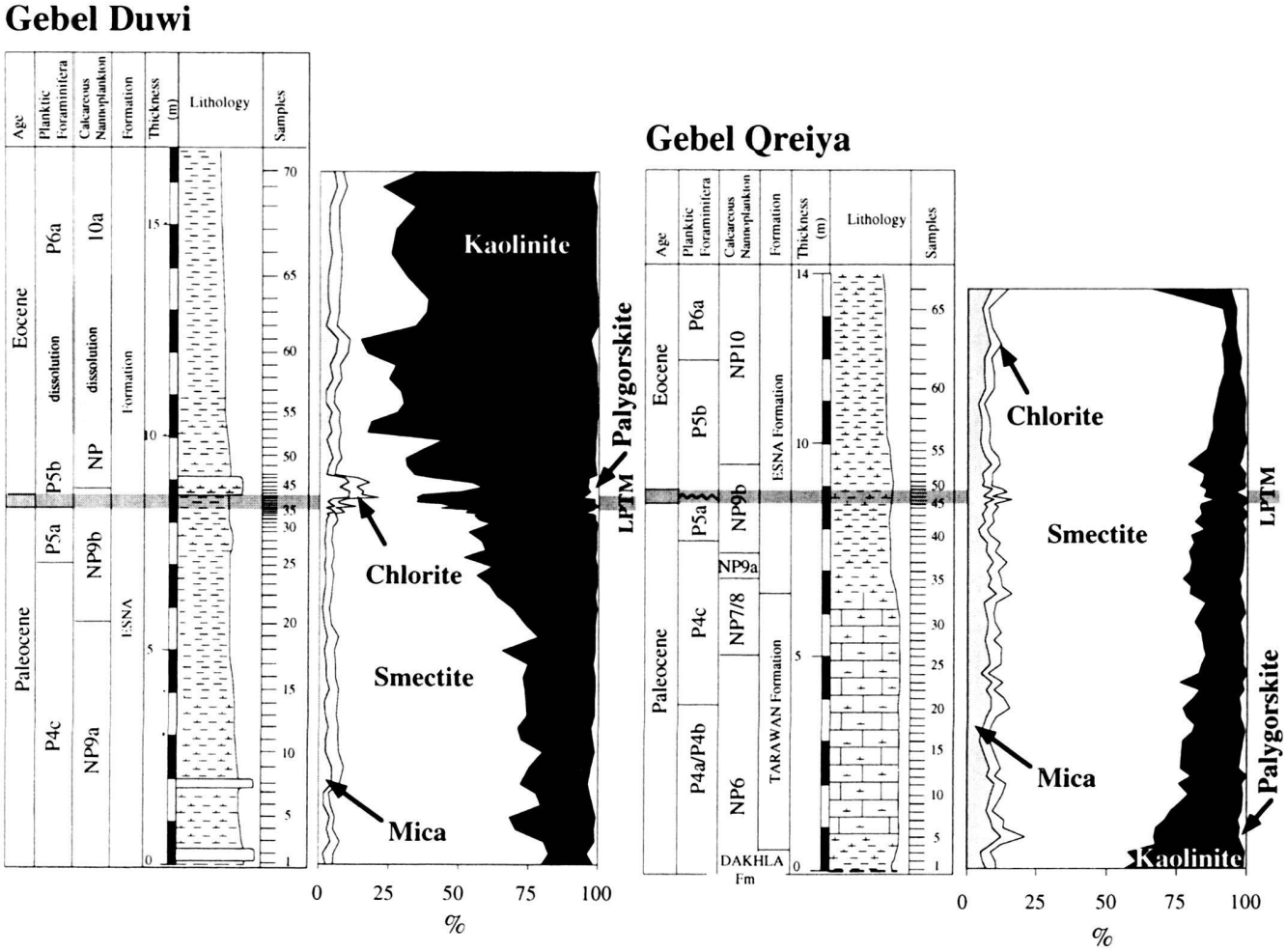

Fig. 7. Clay mineral compositions at Gebel Duwi and Gebel Qreiya (size fraction < 2 μm). Clay minerals are given in relative percent abundance. See Fig. 2 for symbol explanation.

Gebel Qreiya: Calcite is the major component of the sediment throughout the section, averaging 79% (Fig. 5). Phyllosilicates show only minor variations (mean value of 15%) with a maximum value of 42%. Quartz is a minor component of the sediment varying between 1.5% and 3.8%. Dolomite, halite and anhydrite are only sporadically present.

Gebel Matulla: The dominant component is calcite, which averages 77% in the lower part of the section and increases to a maximum of 90% in the limestones between 9 m and 11 m (Fig. 6). Phyllosilicates decrease to near zero in the limestones (Fig. 6). The onset of the LPTM is marked by an abrupt decrease in calcite to 4%, which corresponds to a dissolution interval as indicated by calcareous nannofossils (Fig. 3). This drastic decrease corresponds to an increase in phyllosilicates, in quartz to 9% and the occurrence of potassic feldspar. Above the LPTM interval, calcite gradually decreases whereas phyllosilicates increase. Barite is sporadically present in small amounts in the sediments.

Abu Zenima: From the base to 1.8 m, calcite fluctuates between 75% and 38% (Fig. 6). The LPTM interval is marked by a drastic decrease of calcite to 0%, a concomitant increase in phyllosilicates to 87%, and a high quartz content (12%) and corresponds to a dissolution zone devoid of calcareous nannofossils. Subsequently, calcite recovery is rapid, accompanied by a decrease in phyllosilicates to 23%. Barite is a minor component of the sediments.

The main mineralogical differences between the four sections include the dominance of calcite at Gebel Qreiya, Gebel Matulla and Abu Zenima versus phyllosilicates at Gebel Duwi. In addition phosphate deposition occurs at Gebel Duwi whereas barite is present in the Sinai sections (Gebel Matulla and Abu Zenima). At Gebel Duwi, Gebel Matulla and Abu Zenima, the mineralogical changes which characterize the LPTM are very similar. In these sections, this event is marked by a drastic decrease in calcite coincident with an increase in phyllosilicates and quartz and the occurrence of potassic feldspar

(Sinai sections). Although located between Gebel Duwi and Gebel Matulla, the Gebel Qreiya section shows a completely different bulk rock mineralogical pattern as indicated by the absence of an abrupt decrease in calcite and a strong increase in quartz during the LPTM (Fig. 2).

Clay minerals

Gebel Duwi: Smectite (62%) and kaolinite (31%) dominate the clay mineral fraction (<2μm) in the first 8.2 m (Fig. 7). Mica, chlorite and palygorskite are minor components. The onset of the LPTM event is marked by an increase in kaolinite to 58%. During this event, mica (5.5%), chlorite (5.4%) and palygorskite (2.5%) increase, whereas smectite decreases to a mean value of 28%. The calcarenite bed above the LPTM interval is characterized by a decrease in kaolinite and an increase in smectite, mica and chlorite (Fig. 7). In the upper 8 m, kaolinite averages 70% whereas smectite, mica and chlorite decrease to 22%, 4% and 3% respectively. In this interval, palygorskite content is very low (1%).

Gebel Qreiya: Smectite is the major component throughout the section (Fig. 7). From the base to the top, kaolinite decreases gradually from 40% to 2%. Mica and chlorite contents are relatively constant throughout the section. Palygorskite is very low (<2%). The clay mineral distributions of the LPTM interval are not significantly distinct from those in the rest of the section.

Gebel Matulla: Smectite dominates the clay mineral fraction throughout the section, averaging 70% (Fig. 8). Kaolinite averages 26% in the first lower 4 m and decreases to 2% between 4 m and 14.6 m. Mica (6%) and chlorite (3.5%) contents are relatively constant from the base of the section to 14.6 m except into the limestones where mica averages 17% and chlorite decreases to near zero. The onset of the LPTM is marked by a sharp but short increase in kaolinite to 44%. Above the LPTM interval, mica and chlorite increase respectively to 13% and 23% whereas kaolinite decreases abruptly. Between 16.9 m and the top of the section, kaolinite increases again, averaging 25%. Mixed-layer illite-smectite (IS) content is very low (<0.7%) and goethite, barite and opal-CT are sporadically present throughout the section.

Abu Zenima: Between 0 m and 1.9 m, smectite is the major component, averaging 94% (Fig. 8). The onset of the LPTM is characterized by the occurrence of kaolinite to 79% and a slight increase in chlorite to 8%. From samples 12 to 14, chlorite content is relatively high (~7%) and mica reaches a maximum of 23% at the top of the interval. Above this interval, the decrease in kaolinite coincides with an increase in smectite whereas mica and chlorite content remain high (Fig. 8). IS content is very low (<2%) and barite and opal-CT are sporadically present (Fig. 8). In both Sinai sections, palygorskite has been observed in traces.

A different kaolinite distribution characterizes the four sections. Kaolinite increases at Gebel Duwi from the late Paleocene to the early Eocene, decreases at Qreiya simultaneously and is sporadically present at Gebel Matulla and Abu Zenima, with however, a short-lived strong increase during the LPTM interval. In addition barite and opal-CT are only present in the two Sinai sections. Despite these differences, the four sections show a similar increase in mica and chlorite above the LPTM interval (Figs. 7 and 8).

Geochemistry

Organic matter

Gebel Duwi sediments are poor in organic matter (<0.18%) except for the calcarenite bed which attains 0.3% (Fig. 4): values below <0.2% are considered background noise, consisting of highly refractory organic carbon. The relatively abundant organic matter coincides with the occurrence of apatite (Fig. 4). Gebel Qreiya sediments are extremely poor in organic matter (<0.15%): low values considered as background noise and thus not plotted. In contrast, at Gebel Matulla and Abu Zenima, sediments from the P5b and upper NP9 interval have a relatively high organic carbon content, reaching a maximum of 1.7% (Fig. 9). High organic matter content coincides with the lower $\delta^{13}C$ values measured on the fine fraction (<63μm) of the sediments (Fig. 9).

Stable isotopes

Gebel Duwi: From the base to 8.2 m $\delta^{13}C$ values average –0.5‰ (Fig. 4). The onset of the LPTM interval is marked by a rapid decrease in $\delta^{13}C$ values from – 1.1‰ to –8.8‰. The post-$\delta^{13}C$ shift recovers gradually from –3.7‰ to –1.7‰. High dolomite content generally coincides with the extremely light $\delta^{13}C$ values observed in the first calcarenite bed and at the base of the LPTM interval (Fig. 4).

From the base to the top of the section $\delta^{18}O$ values gradually decrease from –4.1‰ to –6.5‰ with the exception of the calcarenite bed and the base of the LPTM interval where $\delta^{18}O$ values increase to –2.3‰. These relatively "high" $\delta^{18}O$ values coincide also with the presence of dolomite (Fig. 4).

Gebel Qreiya: From the base to 5.2 m, $\delta^{13}C$ values gradually increase from 0.9‰ to 1.7‰ (Fig. 5). $\delta^{13}C$ values decrease to a minimum value of 0.9‰ in the LPTM interval. Above this interval, values increase to 1.2‰ but remain lower than below the LPTM interval (1.7‰). The lower magnitude of the negative $\delta^{13}C$ shift at Gebel Qreiya (~1‰), as compared with 2.5‰-3‰ in other Middle Eastern sections (Lu et al. 1995; Schmitz et al. 1996; Charisi & Schmitz 1995, 1998) suggests the presence of a hiatus which encompasses the lower part of the carbon isotopic excursion.

$\delta^{18}O$ values vary between –2.9‰ and –3.9‰ throughout the section.

Gebel Matulla: From the base to 14.2 m, $\delta^{13}C$ values vary between 0.65‰ and 2.5‰ (Fig. 9). There is a one point negative $\delta^{13}C$ excursion (–5.4‰) near the P5a/b interval, suggesting a hiatus similar to other sections (Fig. 9). A second minimum

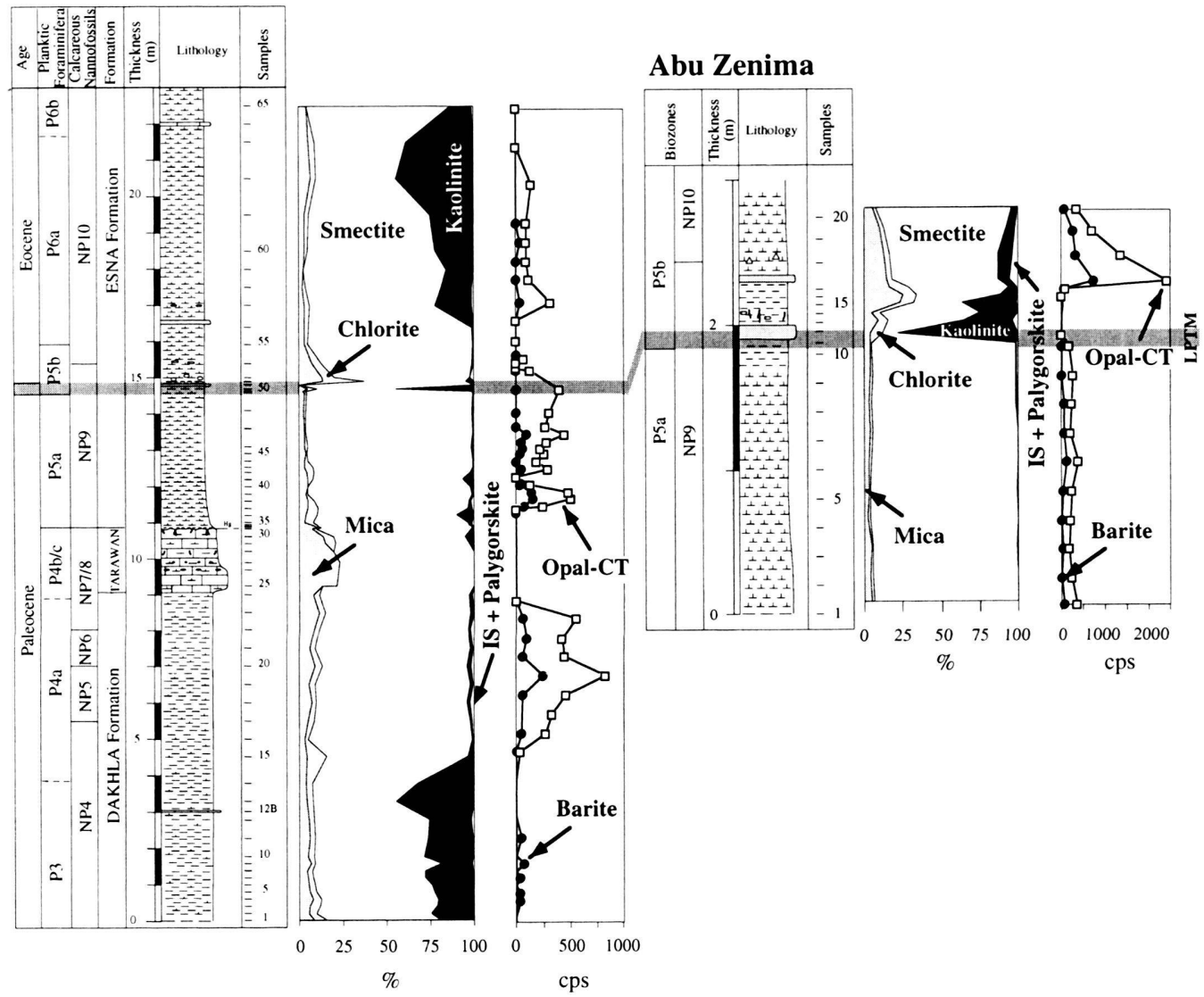

Fig. 8. Clay mineral compositions at Gebel Matulla and Abu Zenima (size fraction < 2 μm). Clay minerals are given in relative percent abundance except for barite and opal-CT given in counts per second (CPS). See Fig. 3 for symbol explanation.

in the $\delta^{13}C$ values is observed (– 2.7‰). Above this interval, $\delta^{13}C$ values vary between –1.3‰ and –0.04‰.

In this section, $\delta^{18}O$ values vary between –11.8‰ and – 3‰ (Fig. 9).

Abu Zenima: The $\delta^{13}C$ record of the Abu Zenima section shows a similar trend across the LPTM interval as observed for the Gebel Matulla section. In the lower part of the section, $\delta^{13}C$ values are constant (0.55‰). An isolated one point negative $\delta^{13}C$ shift of 5.4‰ is observed near the Zone P5a/b boundary with a rapid return to 0.7‰ suggesting a hiatus (Fig. 9). Between 1.9 m and 2.1 m, $\delta^{13}C$ values reach minimum of –2.2‰. Above this minimum, values increase but remain lower than those in the lower part of the section. Overall, $\delta^{18}O$ values vary between –3.6‰ and –10.1‰ throughout the section (Fig. 9).

Discussion

Late Paleocene Thermal Maximum in Egypt

Despite the possibility of a hiatus at the P5a/P5b boundary, as indicated by a single point $\delta^{13}C$ excursion, the characteristic changes of the LPTM interval are well marked in the Egyptian sections. At Gebel Duwi (middle neritic), Gebel Matulla, and Abu Zenima (upper bathyal), this interval is characterized by similar changes. A sudden turnover in the benthic foraminifera

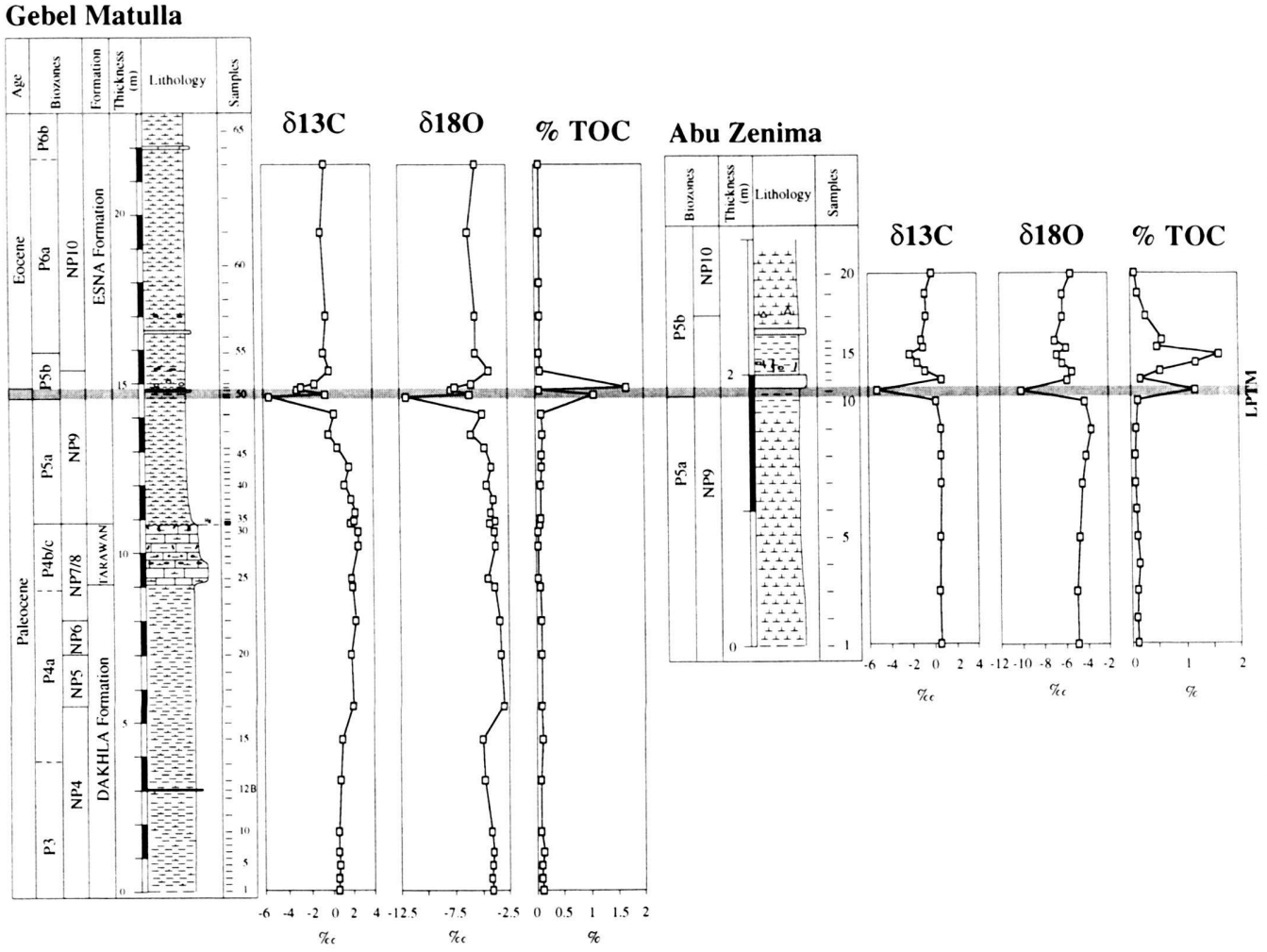

Fig. 9. Stable isotopic and TOC trends at Gebel Matulla and Abu Zenima. Stable isotopes analyses were conducted on the fine fraction (< 63 μm) of the bulk samples. See Fig. 3 for symbol explanation.

marks the BEE (Speijer 1994; Tantawy 1998; Speijer et al. in press) coincident with a major turnover in the calcareous nannofossils (Tantawi 1998) and the first appearance of the characteristic short ranging LPTM species *A. sibaiyaensis*. This faunal turnover is accompanied by decreased calcite and increased detrital quartz and high kaolinite contents. At Gebel Duwi the onset of the LPTM coincides with the 40 cm thick clay interval below the calcarenite bed (Fig. 2). In the Sinai, the critical interval is very condensed (~10 cm thick at Abu Zenima and less than 50 cm at Gebel Matulla) and corresponds to a marly clay layer enriched in organic matter, just below a calcarenite bed (Fig. 3). The abruptness and the extremely rapid recovery from the changes that characterize the LPTM and the low sedimentation rate (reduced thickness of the biozones) suggest condensed sedimentation and/or erosion in the two Sinai sections.

The characteristic trends of the LPTM cannot be identified at Gebel Qreiya where sediments were deposited at an intermediate paleodepth (~200 m). There is no sudden appearance of a large population of *A. sibaiyaensis*, no decrease in calcite, no increase in detritus, no peak in kaolinite and only a very moderate $\delta^{13}C$ shift (~0.3‰). All these observations point toward a significant erosion or non-deposition, and removal of the critical LPTM interval. A greater interval appears to be missing than at Gebel Duwi (Fig. 2). Hiatuses, condensed sedimentation and/or dissolution intervals across the Paleocene-Eocene transition have been observed in many other sections of this region (Lu et al. 1998; Speijer & Schmitz 1998; Bolle 1999; Tantawy et al. 1999).

Diagenetic effects on the isotopic record

The oxygen isotopic data from the four sections indicate extensive diagenetic alteration. The $\delta^{18}O$ values for the fine fraction vary between – 2.3‰ and –11.9‰; most values are in the range –3.5‰ to –5‰ (Figs. 4, 5 and 9). The $\delta^{18}O$ values are sin-

gularly lower than those recorded on well preserved benthic foraminifera from coeval marine Middle East sections (Charisi & Schmitz 1998), but similar to whole-rock $\delta^{18}O$ records overprinted by diagenesis from some Tethyan sections (Corfield et al. 1991; Charisi & Schmitz 1995) suggesting alteration during early diagenesis. Therefore paleoenvironmental interpretations (paleotemperature or salinity indices) using oxygen isotope ratios would be not reliable.

Aissaoui (1985) has measured stable carbon and oxygen isotopes from different carbonate minerals composing Miocene cements from the Red Sea. The most significant feature of the dolomite concerns the depletion in heavy oxygen isotopes (between –3.1 ‰ and –0.7‰) relative to other carbonate minerals (aragonite and calcite). Relatively heavy oxygen isotopic values (between –0.6‰ and 2‰) have also been obtained from middle Eocene dolomites from Egypt (Holail 1994). $\delta^{13}C$ values are relatively low varying between –8‰ and –12‰ in the Miocene dolomitic cement (Aissaoui 1985) and ranging from 1.9‰ to –5.7‰ in the middle Eocene dolomite (Holail 1994). In most coeval marine Middle East sections the BEE coincides with a rapid negative $\delta^{13}C$ excursion of about 3‰ (Lu et al. 1995; Schmitz et al. 1996; Charisi & Schmitz 1995, 1998; Speijer et al. in press). At Gebel Duwi the high magnitude of the negative shift (~7.6‰) suggest that the primary carbon isotope signal is overprinted and accentuated by the early diagenetic dolomite forming, probably as a result of sulfate reduction, at the onset of the LPTM (Fig. 4). Without taking in account the extremely light $\delta^{13}C$ values, the negative $\delta^{13}C$ shift is about 2.7‰ and corresponds to those observed in most latest Paleocene Middle Eastern Tethyan sections.

In both Sinai sections, high TOC coincides with minimum $\delta^{13}C$ values in Subzone P5b and upper Zone NP9 (Fig. 8). This organic material, strongly depleted in ^{13}C, could have contributed to the two negative $\delta^{13}C$ excursions. Based on the faunistic criteria (see p.10), the first $\delta^{13}C$ shift observed seems to be related to the LPTM, whereas the second one is probably an artifact of organic matter influx. However, the high amplitude of the negative LPTM $\delta^{13}C$ shift (5.6‰) indicates that the primary carbon isotopic signal may also be partly overprinted and amplified by the very light carbon isotopic signal of the organic matter.

Compared with the global signal of the LPTM $\delta^{13}C$ shift, all four Egyptian sections reveal a short-term, even single point excursion, which is likely the result of short hiatuses and more negative values probably related to the presence of dolomite (e.g. Gebel Duwi) and high organic matter content (e.g. Gebel Matulla and Abu Zenima).

Significance of clay minerals

Clay minerals and their relative abundance may record information on climate, eustasy, burial diagenesis, or reworking. Detrital input is the dominant factor responsible for the clay mineral distribution in marine sediments. Mica, chlorite, associated quartz and feldspars typically constitute terrigenous species (Chamley 1998). These clay minerals develop generally in areas of steep relief where active mechanical erosion limits soil formation, particularly during periods of enhanced tectonic activity (Millot 1970; Chamley 1998).

Smectite in oceanic sediments can originate from volcanogenic, diagenetic and detrital sources. The sediments in the Egyptian sections did not suffer deep burial diagenesis; the absence of significative diagenetic overprint is documented by the constant but variable presence of smectite, the near absence of mixed-layers illite-smectite, and the co-existence of smectite with a high kaolinite content in different parts of the studied sections (Figs. 7 and 8). Authigenic smectite can form locally in deep-sea environments during hydrothermal weathering of volcanic rocks (Karpoff et al. 1989; Chamley 1998). However, based on the long-term stability of the strontium-isotope records for the Paleocene at Gebel Aweina (paleodepth fluctuations beyond 150 and 200 m; Speijer & Schmitz, 1998), which is located between Gebel Duwi and Gebel Qreiya, Charisi & Schmitz (1995) suggest no major changes in tectonic activity, weathering rates or hydrothermal activity during the Paleocene. This relatively stable period at the southern Tethyan margin indicates that smectite is mainly of detrital origin and may be used as marker of a warm climate, with alternating wet and dry seasons (Chamley 1998). On the other hand, it has been shown that maximum amounts of smectite frequently coincide with long-term or short-term high sea levels (Debrabant et al. 1992; Deconinck 1992). In that case, smectite variations could be also used as indicators of sea level fluctuations.

Increased kaolinite contents in marine sediments result either from increased runoff, which could be caused by sea level falls, or from increased rainfall (Robert & Kennett 1994). This mineral develops in equatorial to tropical soils characterized by a warm, humid climate, well-drained areas with high precipitation and accelerated leaching of parent rocks (Robert & Chamley 1991). But, kaolinite may also be introduced in significant amounts into oceanic sediments through erosion of older sediments and soils containing kaolinite during the sea level rises (Thiry 1989; Chamley 1998). Hendriks et al. (1990) interpreted the presence of kaolinite in Paleogene sediments of Egypt as continental neocrystallizations formed in soils under warm and at least seasonally humid climatic conditions, which have been weathered and transported toward the sea by rivers, the main source of kaolinite being the continental hinterland (Arabian-Nubian shield). The climatic significance of kaolinite in marine sediments of Egypt is consistent with paleobotanical and palynological data which indicate, that subtropical to tropical conditions prevailed onshore during the deposition of the Esna Formation (late Paleocene to early Eocene age; Abou-Ela 1989). Laterization processes and the presence of bauxite observed on the African craton suggest also the dominance of a humid climate and intensive chemical weathering during this period of time (Millot 1970; Hendriks et al. 1990; Robert & Chamley 1991).

Palygorskite and sepiolite have three main origins: (1) These fibrous clay minerals can form during hydrothermal weathering of Mg-bearing rocks, especially those of volcanic origin (Karpoff et al. 1989). However, it has been shown previously that from the late Paleocene to early Eocene the southern Tethyan margin was relatively stable. (2) Palygorskite may form along coastal or peri-marine environments where continental waters are concentrated by evaporation leading to solutions enriched in Si and Mg (Robert & Chamley 1991). This process of neoformation by chemical precipitation is accelerated in warmer zones (Millot 1970; Chamley 1989). (3) Palygorskite but also, to a much lesser extent sepiolite, are frequently found on land in calcareous pedogenic and calcrete soils in arid to semi-arid climatic zones (Chamley 1989; Robert & Chamley 1991).

Hendriks et al. (1990) and Strouhal (1993) noted the coexistence of kaolinite with major occurrences of palygorksite (~25%) and sepiolite (~10%) in the Kharga Oasis area, to the southeast of our studied area. These authors interpreted the presence of these two minerals as neoformations in a warm marine environment in relation with continental weathering under humid climatic conditions.

However, if high precipitation associated with warmer temperatures on the continental hinterland are required to extract magnesium and silicon ions, the chemical elements essential for the crystallization of Mg-rich palygorskite and sepiolite (Hendriks et al. 1990), warm and arid climatic conditions favouring enhanced evaporation and subsequently concentration of magnesium and silicon are necessary to precipitate such clay minerals in coastal basins or peri-marine environments (Robert & Chamley 1991).

Climatic and environmental changes in Egypt

Clay minerals variations in marine sediments of Egypt result from the interdependence between climatic changes on the adjacent continental hinterland, the paleobathymetry, the distance from the shoreline and sea level fluctuations.

During the early Paleocene, the adjacent coastal or continental areas of the southern Tethys margin were influenced by a warm and humid climate with high rainfall as indicated by the abundance of kaolinite observed in oceanic sediments in the Negev area (Arkin et al. 1972; Bolle 1999) and in southern Tunisia (Bolle et al. 1999). These humid climatic conditions are also seen in the sediments in Egypt as indicated by the high kaolinite content observed at the base of the Gebel Matulla section (Zones P3 and NP4). This climatic trend is in agreement with the humid and warm climate that marked the end of the Cretaceous and beginning of the Paleogene in the region (Arkin et al. 1972; Keller et al. 1998; Li et al. in press).

The abundance of smectite and the relatively low kaolinite content observed at Gebel Duwi, located close to the shoreline, suggest a seasonal warm climate with the dominance of wet seasons in the hinterland during the late Paleocene (Subzones P4c and NP9a) (Fig. 7). The gradual increase in kaolinite in the marine sediments of this section indicates the progressive development of humid perennial climatic conditions with high rainfall on the adjacent land area during the latest Paleocene (Subzone P5b), reaching maximum humidity (70% of kaolinite) in the early Eocene (Subzone P6a). High precipitation associated with warm temperatures probably favoured intensive leaching of the parent rocks, formation of kaolinic soils and the development of a subtropical to tropical flora onshore (Abou-Ela 1989).

Similar to other lower latitude Tethys sections (southern Spain and northern Tunisia) (Lu et al. 1998; Bolle et al. 1999), North Atlantic sections (Gibson et al. 1993; Knox et al. 1996; Gawenda et al. 1999) and high latitude sections (Robert & Chamley 1991; Robert & Kennett 1992, 1994; Kaiho et al. 1996), Egyptian sections appear to be affected during the LPTM by an episode of humidity indicated by strong kaolinite influx. This episode of humidity is as well marked in middle neritic environments (Gebel Duwi; Fig. 7) as in upper bathyal environments (Gebel Matulla and Abu Zenima; Fig. 8). However, contrary to other P/E sections where the kaolinite episode is short-lived and restricted to the duration of the LPTM (Robert & Chamley 1991; Robert & Kennett 1992, 1994; Gibson et al. 1993; Kaiho et al. 1996; Knox et al. 1996; Lu et al. 1998; Bolle et al. 1999), humid climatic conditions persisted through the early Eocene in the continental hinterland (Arabian-Nubian shield) of the Egyptian basin, as suggested by the abundance of kaolinite observed at Gebel Duwi (Fig. 7).

Palygorskite and sepiolite have frequently been observed in coastal basins and peri-marine environments of West and North Africa and Israel where the deposition of these two minerals started to increase in the late Paleocene to dominate the clay fraction in the early Eocene. This palygorskite and sepiolite event indicates that some coastal areas experienced intensive aridity and evaporation (Robert 1982; Bolle et al. 1999) whereas humid conditions prevailed on the adjacent continental hinterland (Robert & Chamley 1991). The presence of palygorskite in marine sediments of Egypt suggests an arid climate and enhanced evaporation in the source area where this fibrous clay mineral is formed. The existence of restricted basins between emerged land masses in the Negev area (Israel; Arkin et al. 1972) to the north of our studied area, could be one of the sources for this clay mineral observed in the marine sediments of Egypt.

The distribution of kaolinite and smectite in marine sediments of Egypt appears to be partly related to the distance to the shoreline and to sea level changes. In Subzone P5a and lower NP9b, the kaolinite content decreases from middle neritic to upper bathyal depths, reaching ~45% at Gebel Duwi ~20% at Gebel Qreiya and near 0% at Gebel Matulla and Abu Zenima. A similar decrease has been observed from the top of P5b to the base of P6a and lower NP10 where kaolinite attains ~60%, 20% and 2%, respectively (Figs. 7 and 8). In both cases, the decrease in kaolinite coincides with an increase in smectite (Figs. 7 and 8). Such a clay mineral segregation by

differential settling processes has been commonly observed in Cretaceous sediments where large carbonate platforms grade over a short distance into deep basins (Chamley & Masse 1975; Adatte & Rumley 1984, 1989; Deconinck et al. 1985). The main mechanism responsible for this segregation appears to be grain size sorting, smectite consisting generally of smaller particles than kaolinite (Gibbs 1977; Chamley 1989). Hendriks et al. (1990) and Strouhal (1993) have interpreted a similar kaolinite decrease in the direction to the open sea in the late Paleocene to early Eocene of Egypt as the result of weak oceanic currents.

Based on foraminiferal evidence in middle and southern Egypt, Luger & Schrank (1987) attributed transgressive peaks to the late Paleocene (base of Zone P5) and to the earliest Eocene (upper part of the Esna Formation; *edgari* Zone=≈Subzone P6a in Berggren et al. 1995) whereas the early Eocene corresponds to a regressive event (Fig. 1 in Luger & Schrank 1987).

The coincidence between transgressive episodes affecting Egypt from the late Paleocene to the early Eocene, and the decrease in kaolinite with a corresponding smectite increase toward the open ocean, suggest that during periods of sea level rise kaolinite is preferentially deposited close to shorelines, while smectite is transported away from shorelines.

The re-occurrence of kaolinite (~45%) in the early Eocene (topmost Subzone P6a and lower Zone NP10) observed in the more distal environment (Gebel Matulla) could be related to the regressive period observed in Egypt (Luger & Schrank 1987). During this period of sea level lowering, sediment deposition of Gebel Matulla took probably place in a shallower environment than during the late Paleocene, which becomes favourable to the trapping of kaolinite, whereas smectite is shifted away toward the open sea. However this hypothesis remains speculative because of the non-recovery of Subzone P6b or NP10b in the three other Egyptian sections (Gebel Duwi, Gebel Qreiya, Abu Zenima). Moreover, more detailed studies on the faunistic assemblages are necessary in order to confirm the paleobathymetric evolution of the Sinai region and the sea level fall which affected the early Eocene (Subzone P6b). Although kaolinite distribution in direction of the open sea appears to be related to sea level fluctuations, we cannot exclude that the absence of kaolinite in the sediments of Gebel Matulla (Subzones P4a to P5a) is partly related to climate. The absence of kaolinite and the abundance of smectite observed in Western Sinai could indicate a temperate climate with the dominance of dry seasons, between the more humid and warm climatic conditions prevailing on the African craton to the south, and arid climatic conditions dominating on the peri-marine environments to the north during the late Paleocene (Bolle 1999).

Paleoproductivity changes

Whole rock, benthic and planktic $\delta^{13}C$ values are constantly lower at the southern Tethyan margin (Egypt and Israel) than in other Tethys and Pacific sections (Lu et al. 1995; Charisi & Schmitz 1995, 1998; Schmitz et al. 1996; Bolle 1999). These unusually light $\delta^{13}C$ values have been variously explained by enhanced input of organic matter of terrestrial origin, continental margin upwelling bringing $\delta^{13}C$ –light waters to the surface, reduced surface water biological productivity in relation with increased aridity in peri-marine environments and, paleogeographic restriction of the southern Tethyan margin (Lu et al. 1995; Charisi & Schmitz 1995, 1998; Schmitz et al. 1996; Bolle 1999).

The paleoproductivity and/or paleoceanographic significance of the carbon isotopic trends is considered carefully in this study. Actually real $\delta^{13}C$ values, in particular during the LPTM interval seem to be overprinted by external factors, such as diagenesis and a short hiatus at the LTPM in all sections examined. However, $\delta^{13}C$ values show an increase from the middle neritic to upper bathyal environments during the late Paleocene (Zone P4 and Subzone P5a); At this period, $\delta^{13}C$ values have a mean value of -0.6‰ at Gebel Duwi, average 1.2‰ at Gebel Qreiya whereas higher values (~2‰) have been observed at Gebel Matulla (Figs. 4, 5 and 9). This increase in direction of the open sea suggests two possible scenarios. First, the different $\delta^{13}C$ values could be entirely the result of local diagenetic effects. The sediments in the shallower site (Gebel Duwi) would be more sensitive to diagenetic alteration than the deeper environment (Gebel Matulla). Oberhänsli et al. (1998) have shown that sediments deposited in shallow water environments undergo more drastic alteration than deep water sediments. A second explanation would be that the increase of the $\delta^{13}C$ values toward the open sea has regional significance. Speijer et al. (in press) report a similar gradual positive trend from the neritic sections of Gebel Aweina and Gebel Duwi to the deepest sections (Negev area and Sinai), as reflecting increased restriction from the open sea towards shallower sites and maybe greater influence from the Arabian-Nubian shield. Based on this observation we suspect that a high input of light carbon from the hinterland and its effects might play an important role on the $\delta^{13}C$ signal in the site deposited closest to the adjacent continent (Gebel Duwi), diminishing with the distance from the shoreline (Gebel Matulla). These observations are consistent with the Gebel Aweina section deposited at a paleodepth of about 150–200 m where Charisi & Schmitz (1998) suggest that enhanced input of organic matter of terrestrial origin could be one explanation for the low $\delta^{13}C$ values recorded. Despite the absence of TOC-rich sediments in our sections, except within Subzone P5b and upper NP9 (Figs. 3 and 9), the interpretation of a terrestrial organic matter input inducing the negative $\delta^{13}C$ values cannot be excluded. In fact negative whole-rock $\delta^{13}C$ values by isotopic exchange processes may result from a decrease in pore water $\delta^{13}C$ composition due to dissolved organic matter input in sediments (Zahn et al. 1986; McCorkle et al. 1990).

$\delta^{13}C$ values in the four sections are difficult to compare during the latest Paleocene (Subzones P5b and NP9b) due to the influence of factors which have modified the original carbon isotopic signal (see pp. 44 and 45). However different indicators of high-productivity have been observed in this interval,

within and just above the BEE bed. At Gebel Duwi, the calcarenite bed is characterized by enrichment in phosphates and a relatively high TOC content (0.3%) whereas at Gebel Matulla and Abu Zenima high TOC amounts (~1.8%) associated with iron nodules and fish fossil remains characterize Subzone P5b and upper NP9 (Figs. 3 and 9). A similar organic carbon-rich bed containing fish debris that marks the LPTM interval has been observed by Speijer et al. (1997) in the Wadi Nukhl section (Sinai). Moreover in the Gebel Matulla and Abu Zenima sections, barite and opal-CT, two potential paleoproductivity indicators (Dehaires et al. 1980; Schmitz 1987), are sporadically present throughout the profiles suggesting relatively high productivity from the late Paleocene into the early Eocene in this upper bathyal environment (Fig. 8). The absence of these two minerals in the sediments of Gebel Duwi may be due to the shallower environment of the site. Actually, the accumulation of barite and opal increases with the water depth (Von Breymann et al. 1992; Schmitz et al. 1997). The absence of paleoproductivity indices at Gebel Qreiya in Subzone P5b may be due to the hiatus described previously.

From the late Cretaceous to the Eocene, intermittent upwelling episodes must have affected the southern margin of the Tethys (Almogi-Labin et al. 1993). The long-term evolution of this upwelling system is recorded in the widespread late Cretaceous to Eocene phosphate belt that extends from South America through North Africa as far as the Arabian Craton (Almogi-Labin et al. 1993). In Egypt, the main phosphate accumulations are late Campanian to early Maastrichtian in age (Duwi Formation; Youssef 1957; Kamel 1982; Glenn 1990; Glenn & Arthur 1990). The presence of the phosphates observed in the calcarenite bed above the BEE at Gebel Duwi, suggests the two following scenarios. First, phosphate accumulation may be the result of erosion from underlying upper Cretaceous phosphate-rich sediments. Phosphorite deposits from the late Cretaceous Duwi Formation consist mainly of phosphatized peloids and skeletal grains (phosphatized or primary fish debris). These upper Cretaceous phosphorites are interbedded with glauconite-rich greensands (Glenn 1990). However, the absence of glauconitic particles, no reworked Cretaceous calcareous nannofossils, a planktic foraminifera packing and alternating poor phosphatic grains microbeds with rich-phosphatic particles layers in the calcarenite bed of Gebel Duwi, all point toward a condensation origin of the phosphates (Föllmi, pers. communication 1999) rather than an allochthonous origin from upper Cretaceous sediments. Second, the latest Paleocene (Subzone P5b) corresponds to a period of phosphate deposition and consequently of high nutrient input. Condensed phosphates are more or less autochthonous, but have experienced one or more phases of current winnowing, erosion and reworking (Föllmi 1996). Moreover, this type of phosphates is preferentially accumulated along maximum flooding surfaces (Föllmi et al. 1992; Föllmi 1996). The presence of phosphates in the calcarenite of Gebel Duwi suggests a maximum of transgression in Subzone P5b and upper Zone NP9. The increase of smectite, mica and chlorite in the calcarenite bed (Fig. 7) is consistent with a transgressive event. High smectite amounts frequently coincide with short-term high sea levels (Debrabant et al. 1992; Deconinck 1992) whereas reworking and condensation favour the accumulation of mica and chlorite. This transgressive episode deduced from the presence of a condensed phosphatic bed and high smectite, mica and chlorite contents is in agreement with the deepening of the Egyptian basin in the upper part of Zone P5, based on sedimentologic and biotic evidences reported by Speijer et al. (1996) and Speijer & Schmitz (1999).

Two mechanisms may be invoked to explain the high-nutrient input and consequently the phosphate deposition observed at the end of the Paleocene (Subzones P5b and NP9b) at the shallower Gebel Duwi site. First an upwelling episode which is one of the best-known and most efficient ways of supplying nutrients (Lucas & Prévôt-Lucas 1997). During the late Paleocene the southern Tethyan margin was affected by upwelling processes indicated mainly by the occurrence of radiolarian, benthic foraminifera data and geochemical proxies (Benjamini 1992; Speijer & Van der Zwaan 1994; Lu et al. 1995; Schmitz et al. 1997; Charisi & Schmitz 1998). However, a controversy persists as for the cessation (Lu et al. 1995) or the intensification (Speijer & Van der Zwaan 1994; Speijer et al. 1996, 1997; Schmitz et al. 1997) of this upwelling activity during the LPTM interval. The co-existence of upper bathyal organic-rich sediments (Gebel Matulla) and middle neritic phosphate deposits (Gebel Duwi) in Subzones P5b and NP9b just after the BEE could confirm an upwelling activity during this period. In fact such a lateral segregation into different depositional belts is analogous to several modern upwelling environments where diatomaceous muds, often rich in phosphates, are confined to the inner shelf, while organic-rich sediments accumulate further offshore (Summerhayes 1983; Suess et al. 1990). By analogy the deposition in the Sinai and at Gebel Duwi could reflect their position relative to the upwelling center. At the maximum peak of upwelling during the latest Paleocene, the inner belt (represented by the shallower site, Gebel Duwi) was more productive than the outer, offshore belt (Sinai). During this upwelling activity, lateral currents caused winnowing affecting the inner shelf (Gebel Duwi) reducing the sediment accumulation and leading to the condensation of phosphates.

Second, fluvial input of phosphorus onto the Egyptian shelf may have played a role for the phosphate enrichment into the calcarenite bed of Gebel Duwi. The warm and humid climate with high rainfall inferred from clay minerals which prevailed at the end of the Paleocene on the continental hinterland favoured intensive continental weathering and the release of suspended magnesium, silicon (see p. 45) and probably phosphorus. Although part of the phosphorus can result from intensive weathering and subsequent fluvial discharge into the Egyptian shelf, the presence of organic-rich sediments in the upper bathyal environment in Subzone P5b hardly support this scenario.

Conclusions

Based on sedimentologic, biostratigraphic, mineralogical and geochemical criteria, the following conclusions can be drawn.

1° Clay mineral distribution indicates the dominance of alternating wet and dry seasons during the late Paleocene (Zones P4 to P5a and NP4 to lower NP9). Warm and humid climates with high rainfall initiated during the LPTM (Subzone P5b and upper NP9) and extended into the Eocene (Zone P6 and lower NP10) on the Arabian-Nubian shield.

2° Clay mineral segregation by differential settling intensified during periods of sea level rise.

3° The increase in $\delta^{13}C$ values toward the open sea during the late Paleocene might confirm the hypothesis of light carbon input from the hinterland as being partly responsible for the low negative $\delta^{13}C$ values measured at the southern Tethyan margin.

4° The latest Paleocene in Egypt (Subzone P5b and upper NP9) is marked by a transgressive episode and the accumulation of condensed phosphates in the middle neritic environment. Upwelling activity appears to be the most plausible way for supplying nutrients into this shallower site although part of the phosphorus could have a fluvial source.

5° Our oxygen isotopic data reflect primarily extensive diagenetic alteration. Paleoenvironmental interpretations (paleotemperature or salinity indices) using oxygen isotope ratios are therefore unreliable.

6° All four sections reveal short hiatuses (erosion and/or non-deposition) at the planktic foraminiferal Subzone P5a/b boundary and uppermost part of NP9b, as indicated by the rarity or absence of the P5b index species *A. sibaiyaensis* and short single-point negative carbon excursions.

Acknowledgements

We sincerely thank R. Speijer (Bremen) and K. Von Salis (Zürich) for a stimulating review of the manuscript. We thank J.Richard for conducting X-ray preparations and S. Ryser for conducting total organic carbon measurements at the laboratory of mineralogy and petrology, University of Neuchâtel, Switzerland. We also thank Gerta Keller, Dpt. of Geosciences, Princeton University, USA for providing important comments and suggestions on an early draft. This study was supported by the Swiss National Science Foundation, N°2100-043450.95/1 and by the Egyptian Science and Technology Joint Fund in cooperation with U.S State Dpt. and the Egyptian Ministry of Scientific Research under Project OTH2-008-001-98.

REFERENCES

ABOU-ELA, N.M. 1989: Lower Tertiary microflora from the Esna shale of the Red Sea coast, Egypt. Rev. Esp. Micropal. 21, 189–206.

ADATTE, T. & RUMLEY, G. 1984: Microfaciès, minéralogie, stratigraphie et évolution des milieux de dépôts de la plate-forme berriaso-valanginienne des régions de Sainte-Croix (VD), Cressier et du Landeron (NE). Bull. Soc. neuchâtel. Sci. nat. 107, 221–239.

– 1989: Sedimentology and mineralogy of Valanginian and Hauterivian in the stratotypic region (Jura mountains, Switzerland). In: Cretaceous of the Western Tethys (Ed. by WIEDEMANN, J.). Proc. 3rd Int. Cretaceous Symp., Tübingen, 1987, 329–351.

ADATTE, T., STINNESBECK, W. & KELLER, G. 1996: Lithostratigraphic and mineralogic correlations near the K/T boundary clastic sediments in northeastern Mexico: Implications for origin and nature of deposition. GSA, Spec. Pap. 307, 211–226.

AISSAOUI, D.M. 1985: Botryoidal aragonite and its diagenesis. Sedimentology 32, 345–361.

ALMOGI-LABIN, A., BEIN, A. & SASS, E. 1993: Late Cretaceous upwelling system along the southern Tethys margin (Israel): interrelationship between productivity, bottom water environments, and organic matter preservation. Paleoceanography 8(5), 671–690.

ANGORI, E. & MONECHI, S. 1996: High-resolution nannofossil biostratigraphy across the Paleocene/Eocene bounary at Caravaca (southern Spain). Israel J. of Earth Sci. 44, 197–206.

ARKIN, Y., NATHAN, Y. & STARINSKY, A. 1972: Paleocene-Eocene environments of deposition in the northern Negev (southern Israel). Geol. Survey Israel, Bull. 56, 1–18.

AUBRY, M.-P. 1996: Towards an upper Paleocene-lower Eocene high resolution stratigraphy based on calcareous nannofossil stratigraphy. Israel J. of Earth Sci. 44(4), 239–253.

AUBRY, M.-P. & REQUIRAND, C. 1999: The *Rhomboaster-Tribrachiatus* lineage: a remarkable moment in the evolution of the calcareous nannoplankton. Int. Early Paleogene warm climates and biosphere dynamics Meet., Göteborg, June 9–13, 1999, abstract.

AUBRY, M.-P., BERGGREN, W.A., STOTT, L.D. & SINHA, A. 1996: The upper Paleocene-lower Eocene stratigraphic recorded and the Paleocene/Eocene boundary carbon isotope excursion: implications for geochronology. In: Correlation of the Early Paleogene in Northwest Europe (Ed. by KNOX, R.O.B., CORFIELD, R. & DUNAY, R.E.). Geol. Soc. (London) Spec. Publ. 101, 353–380.

BENJAMINI, C. 1992: The Paleocene-Eocene boundary in Israel: A candidate for the boundary stratotype. N. Jb. Geol. Paläont. Abh. 186, 49–61.

BERGGREN, W.A., KENT D.V., SWISHER III, C.C. & AUBRY, M.P. 1995: A revised Cenozoic Geochronology and Chronostratigraphy. In: Geochronology, time scale and global stratigraphy correlation (Ed. by BERGGREN, W.A., KENT, D.V., AUBRY, M.-P. & HARDENBOL, J.). Tulsa, Oklahoma, USA: SEPM Spec. Publ. 54, 129–213.

BOLLE, M.P., ADATTE, T., KELLER, G., VON SALIS, K. & BURNS, S. 1999: The Paleocene-Eocene transition in the Southern Tethys (Tunisia): Climatic and environmental fluctuations. Bull. Soc. géol. France 170(5), 661–680.

BOLLE, M.P. 1999: Climatic and environmental changes in the Tethys region during the late Paleocene thermal maximum. PhD Thesis, Univ. Neuchâtel, Switzerland, 411p.

BRALOWER, T.J., ZACHOS, J.C., THOMAS, E., PARROW, M., PAUL, C.K., KELLY, D.C., PREMOLI SILVA, I., SLITER, W.V. & LOHMANN, K.C. 1995: Late Paleocene to Eocene paleoceanography of the equatorial Pacific Ocean: Stable isotopes recorded at Ocean Drilling Program Site 865, Allison Guyot. Paleoceanography 10, 841–865.

BRAMLETTE, M.N. & SULLIVAN, F.R. 1961: Coccolithophorids and related nannoplankton of the Early Tertiary in California. Micropaleontol. 7, 129–174.

BYBELL, L.M. & SELF-TRAIL, J.M. 1995: Evolutionary, Biostratigraphic, and Taxonomic Study of calcareous nannofossils from a continuous Paleocene/Eocene boundary section in New Jersey. U.S. Geol. Surv. Prof. Pap. 1554, 1–36.

– 1997: Late Paleocene and Early Eocene calcareous nannofossils from three boreholes in an onshore-offshore transect from New Jersey to the Atlantic Continental Rise. Proc. ODP, Sci. Res. 150, 91–110.

CHAMLEY, H. & MASSE, J.-P. 1975: Sur la signification des minéraux argileux dans les sédiments barrémiens et bédouliens de Provence (SE de la France). 9ème Congr. Int. Sédimentol., Nice, 1, 25–30.

CHAMLEY, H. 1989: Clay sedimentology. Springer-Verlag, Berlin Heidelberg, 623p.

– 1998: Clay Mineral Sedimentation in the Ocean. In: Soils and Sediments (Mineralogy and Geochemistry) (Ed. by PAQUET, H. & CLAUER, N.). Springer-Verlag, Berlin Heidelberg, 269–302.

CHARISI, S. & SCHMITZ, B. 1995: Stable ($\delta^{13}C$, $\delta^{18}O$) and strontium ($^{87}Sr/^{86}Sr$) isotopes through the Paleocene at Gebel Aweina, eastern Tethyan region. Palaeogeogr. Palaeoclimatol. Palaoecol. 116, 103–129.

– 1998: Paleocene to early Eocene paleoceanography of the Middle East: The $\delta^{13}C$ and $\delta^{18}O$ isotopes from foraminiferal calcite. Paleoceanography 13(1), 106–118.

CORFIELD, R.M., CARTLIDGE, J.E., PREMOLI-SILVA, I. & HOUSLEY, R.A. 1991: Oxygen and carbon isotope stratigraphy of the Paleogene and Cretaceous limestones in the Bottacione Gorge and the Contessa Highway sections, Umbria, Italy. Terra Nova 3, 414–422.

DEBRABANT, P., FAGEL, N., CHAMLEY, H., DECONINCK, J.F., RERCOURT, P. & TROUILLET, A. 1992: Clay Sedimentology, mineralogy and chemistry of Mesozoic sediments drilled in the northern Paris Basin. Sci. Drill. 3, 138–152.

DECONINCK, J.F. 1992: Sédimentologie des argiles dans le Jurassique-Crétacé d'Europe occidentale et du Maroc. Mém. Habilitation, Univ. Lille I, 226p.

DECONINCK, J.F., BEAUDOIN, B., CHAMLEY, H., JOSEPH, P. & RAOULT, J.-F. 1985: Contrôles tectonique, eustatique et climatique de la sédimentation argileuse du domaine subalpin français au Malm-Crétacé. Rev. Géogr. Phys. Geol. Dyn. 26, 311–320.

DEHAIRES, F., CHESSELET, R. & JEDWAB, J. 1980: Discrete suspended particles of barite and the barium cycle in the ocean. Earth and Planet. Sci. Lett. 49, 528–550.

FERRERO, J. 1966: Nouvelle méthode empirique pour le dosage des minéraux par diffraction RX. Rapport C.F.P (Bordeaux) inédit, 26.

FÖLLMI, K., GARRISON, R.E., RAMIREZ, P.C., ZAMBRANO-ORTIZ, F., KENNEDY, W.J. & LEHNER, B.L. 1992: Cyclic phosphate-rich successions in the upper Cretaceous of Colombia. Palaeogeogr. Palaeoclimatol. Palaeoecol. 93, 151–182.

FÖLLMI, K. 1996: The phosphorus cycle, phosphogenesis and marine phosphate-rich deposits. Earth-Sci. Rev. 40, 55–124.

GAWENDA, P., WINKLER, W., SCHMITZ, B. & ADATTE, T. 1999: Climate and bioproductivity control on carbonate turbidite sedimentation (Paleocene to earliest Eocene Gulf of Biscay, Zumaia). J. Sed. Res. 69, 1253–1261.

GIBBS, R.J. 1977: Clay mineral segregation in the marine environment. J. Sed. Petr. 47, 237–243.

GIBSON, T.G., BYBELL, L.M. & OWENS, J.P. 1993: Latest Paleocene lithologic and biotic events in neritic deposits of southwestern New Jersey. Paleoceanography 8, 495–514.

GLENN, C.R. 1990: Depositional sequences of the Duwi, Sibâîya and Phosphate Formations, Egypt: phosphogenesis and glauconitization in a Late Cretaceous epeiric sea. In: Phosphorite Research and Development (Ed. by NOTHOLT, A.J.G. & JARVIS, I.). Geol. Soc. (London) Spec. Publ. 52, 205–222.

GLENN, C.R. & ARTHUR, M.A. 1990: Anatomy and origin of a Cretaceous phosphorite-greensand giant, Egypt. Sedimentology 37, 123–154.

HENDRIKS, F., LUGER, P. & STROUHAL, A. 1990: Early Tertiary Marine Palygorskite and Sepiolite Neoformation in SE Egypt. Z. dtsch. geol. Ges. 141, 87–97.

HOLAIL, H. 1994: Carbon and oxygen ratios of Middle Eocene dolomite, Gebel Ataqa, Egypt. N. Jb. Geol. Paläont. Abh. 191(1), 111–124.

KAIHO, K., ARINOBU, T., ISHIWATARI R., MORGANS, H.E.G., OKADA, H., TAKEDA, N., TAZAKI, K., ZHOU, G., KAJIWARA, Y., MATSUMOTO, R., HIRAI, A., NIITSUMA, N. & WADA, H. 1996: Latest Paleocene benthic foraminiferal extinction and environmental changes at Tawanui, New Zealand. Paleoceanography 11, 447–465.

KAMEL, O.A. 1982: Origin of the Egyptian phosphorites. Ann. Geol. Survey Egypt XII, 237–254.

KARPOFF, A.M., LAGABRIELLE, Y., BOILLOTT, G. & GIRARDEAU, J. 1989: L'authigenèse océanique de palygorskite, par halmyrolyse de péridotites serpentinisées (marge de Galice): ses implications géodynamiques. C.R. Acad. Sci. Paris 308, 647–654.

KELLER, G., ADATTE, T., STINNESBECK, W., STUBEN, D., KRAMAR, U., BERNER, Z. & VON SALIS, K. 1998: The Cretaceous-Tertiary transition on the shallow Saharan Platform of southern Tunisia. Geobios 30, 951–975.

KELLY, D.C., BRALOWER, T.J., ZACHOS, J.C., PREMOLI SILVA, I. & THOMAS, E. 1996: Rapid diversification of planktonic foraminifera in the tropical Pacific (ODP Site 865) during the late Paleocene thermal maximum. Geology 24, 423–426.

KENNETT, J.P. & STOTT, L.D. 1990: Proteus and Proto-Oceanus: Paleogene oceans as revealed from Antartica stable isotopic results. Proc. ODP, Sci. Res. 113, 865–879.

– 1991. Abrupt deep-sea warming, palaeoceanographic changes and benthic extinctions at the end of the Paleocene. Nature 353, 225–229.

KLOOTWIJK, C.T., GEE, J.S., PEIRCE, J.W., SMITH, G.M. & MCFADDEN, P.L. 1992: An early India-Asia contact: Paleomagnetic constraints from Ninetyeast Ridge, ODP Leg 121. Geology 20, 395–398.

KNOX, R.W. 1996: Correlation of the early Paleogene in northwest Europe: an overview. In: Correlation of the Early Paleogene in Northwest Europe (Ed. by KNOX, R.W., CORFIELD, R.M. & DUNAY, R.E.). Geol. Soc. (London) Spec. Publ. 101, 1–11.

KÜBLER, B. 1983: Dosage semi-quantitatif des minéraux majeurs des roches sédimentaires par diffraction X. Cah. Inst. Géol. Neuchâtel Série AX N°1.1 & 1.2.

– 1987: Cristallinité de l'illite, méthodes normalisées de préparations, méthodes normalisées de mesures. Cah. Inst. Géol. Neuchâtel Série ADX, 1–8.

LI, L., KELLER, G., ADATTE, T. & STINNESBECK, W. in press: Late Cretaceous sea level fluctuations in the southwestern Tethys Ocean: a multidisciplinary approach. J. Geol. Soc. London.

LU, G., KELLER, G., ADATTE, T. & BENJAMINI, C. 1995: Abrupt change in the upwelling system along the southern margin of Tethys during the Paleocene-Eocene transition event. Israel J. of Earth Sci. 44, 185–196.

LU, G., KELLER, G., ADATTE, T., ORTIZ, N. & MOLINA, E. 1996: Long-term (10^5) or short-term (10^3) $\delta^{13}C$ and $\delta^{18}O$ excursion near the Palaeocene-Eocene transition: evidence from the Tethys. Terra Nova 8, 347–355.

LU, G., KELLER, G. & PARDO, A. 1998: Stability and change in Tethyan planktic foraminifera across the Paleocene-Eocene transition. Mar. Micropaleontol. 35, 203–233.

LUCAS, J. & PRÉVÔT-LUCAS, L. 1997: On the Genesis of Sedimentary Apatite and Phosphate-rich Sediments. In: Soil and Sediments (Mineralogy and Geochemistry) (Ed. by PAQUET, H. & CLAUER, N.). Springer-Verlag, Berlin, 249–268.

LUGER, P. & SCHRANK, E. 1987: Mesozoic to Paleogene transgressions in middle and southern Egypt-Summary of paleontological evidence. In: Current research in African earth sciences (Ed. by MATHEIS & SCHANDELMEIER). Balkema, Rotterdam, 199–202.

MARTINI, E. 1971: Standard Tertiary and Quaternary calcareous nannoplankton zonation. In: Proc. 2nd Planktonic Conference (Ed. by FARINACCI, A.). Roma: Tecnoscienza, 739–785.

MCCORKLE, D.C., KEIGWIN, L.D., CORLISS, B.H. & EMERSON, S.R. 1990: The influence of microhabitats on the carbon isotopic composition of deep-sea benthic foraminifera. Paleoceanography 5, 161–185.

MILLOT, G. 1970: Geology of Clays. Springer-Verlag, New York, 499p.

MONECHI, S. & THIERSTEIN, H. 1985: Late Cretaceous-Eocene nannofossil and magnetostratigraphic correlations near Gubbino, Italy. Mar. Micropaleontol. 9, 419–440.

MONECHI, S., ANGORI, E. & SPEIJER, R. 1999: Upper Paleocene Stratigraphy: northern versus southern Tethys. Int. Early Paleogene warm climates and biosphere dynamics Meet., Göteborg, June 9–13, 1999, abstract.

OBERHÄNSLI, H. & HSÜ, K.J. 1986: Paleocene-Eocene paleoceanography. In: Mesozoic and Cenozoic Oceans. Geodynamic Series 15, 85–100.

OBERHÄNSLI, H. 1992: The Influence of the Tethys on the bottom waters of the early Tertiary ocean. In: The Antarctic Paleoenvironment: A Perspective on Global Change (Ed. by KENNETT, J.P.), 167–184.

OBERHÄNSLI, H., KELLER, G., ADATTE, T. & PARDO, A. 1998: Diagenetically and environmentally controlled changes across the K/T transition at Koshak, Mangyshlak (Kazakhstan). Bull. Soc. géol. France 169, 493–501

OKADA, H. & BUKRY, D. 1980: Supplementary modification and introduction of code numbers to the low-latitude coccolith biostratigraphic zonation (Bukry, 1973, 1975). Mar. Micropaleontol. 5(3), 321–325.

PARDO, A. & KELLER, G. 1996: Low latitude planktic foraminiferal incursion at the P/E Boundary in the Eastern Boreal Paratethys (Kaurtakapy section, Kazakstan). Int. Paleogene Stage Boundaries Meet., Zaragoza, June 24–29, 1996, abstract.

PARDO, A., KELLER, G. & OBERHÄNSLI, H. 1999a: Paleoecologic and paleoceanographic evolution of the Tethyan realm during the Paleocene-Eocene transition. J. foram. Res. 29, 37–57.

PARDO, A., BOLLE, M.P. & KELLER, G. 1999b: El evento bio-climatico del transito P-E en el Paratethys boreal: datos de $\delta^{13}C$, $\delta^{18}O$ y foraminiferos planctonicos. Rev. Esp. Micropal. 31, 91–96.

PERCH-NIELSEN, K. 1985: Cenozoic calcareous nannofossils. In: Plankton stratigraphy (Ed. by BOLLI, H. M., SAUNDERS, J.B. & PERCH-NIELSEN, K.). Cambridge University Press, 422–454.

RAYMO, M.E. & RUDDIMAN, W.F. 1992: Tectonic forcing of Late Cenozoic climate. Nature 359, 117–122.

ROBERT, C. 1982: Modalité de la sédimentation argileuse en relation avec l'histoire géologique de l'Atlantique Sud. PhD Thesis, Univ. Aix-Marseille II, France.

ROBERT, C. & CHAMLEY, H. 1991: Development of early Eocene warm climates, as inferred from clay mineral variations in oceanic sediments. Palaeogeogr. Palaeoclimatol. Palaeoecol. 89, 315–332.

ROBERT, C. & KENNETT, J.P. 1992: Paleocene and Eocene kaolinite distribution in the South Atlantic and Southern Ocean: Antarctic climatic and paleoceanographic implications. Marine Geology 103, 9–110.

– 1994: Antarctic subtropical humid episode at the Paleocene-Eocene boundary: Clay-mineral evidence. Geology 22, 211–214

ROMEIN, A.J.T. 1979: Lineages in early Paleocene calcareous nannoplankton. Utrecht Micropaleontol. Bull. 22, 18–22.

SAID, R. (editor) 1990: The geology of Egypt. Balkema, Rotterdam, Netherlands, 734pp.

SCHMITZ, B. 1987: Barium, equatorial high productivity and the northward wandering of the Indian continent. Paleoceanography 2, 63–77.

SCHMITZ, B., SPEIJER, R.P. & AUBRY, M.-P. 1996: Latest Paleocene benthic extinction event on the southern Tethyan shelf (Egypt): Foraminiferal stable isotopic ($\delta^{13}C$, $\delta^{18}O$) records. Geology 24, 347–350.

SCHMITZ, B., CHARISI, S., THOMPSON, E.I. & SPEIJER, R.P. 1997: Barium, SiO_2 (excess), and P_2O_5 as proxies of biological productivity in the Middle East during the Palaeocene and the latest Palaeocene benthic extinction event. Terra Nova 9, 95–99.

SELVERSTONE, J. & GUTZLER, D.S. 1993: Post-125 Ma carbon storage associated with continent-continent collision. Geology 21, 885–888.

SPEIJER, R.P. 1994: Extinction and recovery patterns in benthic foraminiferal paleocommunities across the Cretaceous/Paleogene and Paleocene/Eocene boundaries. PhD Thesis, Univ. Utrecht, Netherlands, Geologica Ultraiectina 124, 1–191.

SPEIJER, R.P. & VAN DER ZWAAN, G.J. 1994: The differential effect of the P/E boundary event on extinction and survivorship in shallow to deep water Egyptian benthic foraminiferal assemblages. Geologica Ultraiectina 124, 121–168.

SPEIJER, R.P., VAN DER ZWAAN, G.J. & SCHMITZ, B. 1996: The impact of the Paleocene/Eocene boundary events on middle neritic benthic foraminiferal assemblages from Egypt. Mar. Micropaleontol. 28, 99–132.

SPEIJER, R.P., SCHMITZ, B. & VAN DER ZWAAN, G.J. 1997: Benthic foraminiferal extinction and repopulation in response to latest Paleocene Tethyan anoxia. Geology 25, 683–686.

SPEIJER, R.P. & SCHMITZ, B. 1998: A benthic foraminiferal record of Paleocene sea-level changes and trophic conditions at Gebel Aweina, Egypt. Palaeogeogr. Palaeoclimatol. Palaeocol. 137, 79–101.

– 1999: Paleocene events and sea-level history in the Tethyan epicontinental basin. Int. Early Paleogene warm climates and biosphere dynamics Meet., Göteborg, June 9–13, 1999, abstract.

SPEIJER, R.P., SCHMITZ, B. & LUGER, P. in press: Stratigraphy of late Palaeocene events in the Middle East: implications for low- to middle-latitude successions and correlations. J. Geol. Soc. London.

STROUHAL, A. 1993: Tongeologische Entwicklungstrend in kretazischen and tertiären Sedimenten Nordostafrikas: regional Fallbeispiele. Berliner geowiss. Abh. 155, 1–68.

SUESS, E. et al. (eds). 1990: Proc. ODP. Sci. Res. 112, 1–738.

SUMMERHAYES, C.P. 1983: Sedimentation of organic matter in upwelling regimes. In: Coastal Upwelling, Its Sediment Record, Part B, Sedimentary Records of Ancient Coastal Upwelling (Ed. by THIEDE, J. & SUESS, E.). NATO Conf. Ser. 4, 29–72.

TANTAWY, A.A. 1998: Stratigraphical and paleontological studies on some Paleocene-Eocene successions in Egypt. Ph.D Thesis, Aswan Faculty of Science, South Valley University, Egypt, 273p.

TANTAWY, A.A., OUDA, K., VON SALIS, K. & SAAD EL-DIN, M. 1999: Paleocene biostratigraphy of Egypt. Int. Early Paleogene warm climates and biosphere dynamics Meet., Göteborg, June 9–13, 1999, abstract.

THIRY, M. 1989: Geochemical Evolution and Paleoenvironments of the Eocene continental Deposits in the Paris Basin. Palaeogeogr. Palaeoclimatol. Palaeoecol. 70, 153–165.

THOMAS, E. 1990: Late Cretaceous through Neogene deep-sea benthic foraminifers (Maud Rise, Weddell Sea, Antarctica). Proc. ODP. Sci. Res. 113, 571–594.

THOMAS, E. & SHACKLETON, N. 1996: The Paleocene-Eocene benthic foraminiferal extinction and stable isotope anomalies. In: Correlation of the Early Paleogene in Northwest Europe (Ed. by KNOX, R.W., CORFIELD, R.M. & DUNAY, R.E.). Geol. Soc. (London) Spec. Publ. 101, 401–441.

VON BREYMANN, M.T., EMEIS, K.C. & SUESS, E. 1992: Water depth and diagenetic constrains on the use of barium as a palaeoproductivity indicator. In: Upwelling Systems: Evolution Since the Early Miocene (Ed. by SUMMERHAYES, C.P., PRELL, W.L. & EMEIS, K.C.). Geol. Soc. (London) Spec. Publ. 64, 273–284.

VON SALIS, K., OUDA, K., SAAD EL DIN, M., TANTAWY, A.A. & BERNASCONI, S. 1998: Calcareous nannofossils, foraminifera and stable isotope studies from the P/E boundary sections in Egypt. In: La Limite Paléocène/Eocène en Europe: Evènements et Corrélations (Abstract). Univ. Paul-Sabatier-Toulouse III, Strata 9, Sér.1, 113–115.

VON SALIS, K., MONECHI, S., BYBELL, L.M., SELF-TRAIL, J. & YOUNG, J. 1999: *Rhomboaster/Tribrachiatus*-Calcareous nannofossil markers at the Paleocene/Eocene boundary: a base for discussion. Int. Early Paleogene warm climates and biosphere dynamics Meet., Göteborg, June 9–13, 1999, abstract.

WEI, W. & ZHONG, S. 1996: Taxonomic and magnetobiochronology of *Tribrachiatus* and *Rhombaster*, two genera of calcareous nannofossils. J. Palaeontol. 70, 7–22.

WEI, W. & WISE, S.W. 1989: Paleogene calcareous nannofossil magnetobiochronology: results from South Atlantic DSDP Site 516. Mar. Micropaleontol. 14, 119–152.

YOUSSEF, M.I. 1957: Upper Cretaceous rocks in Quseir area. Bull. Inst. Desert Egypt 7, 35–54.

ZACHOS, J., LOHMANN, K., WALKER, J.C.G. & WISE, S.W. 1993: Abrupt climate change and transient climates during the Paleogene: A marine perspective. J. Geol. 101, 191–123.

ZAHN, R., WINN, K. & SARNTHEIN, M. 1986: Benthic foraminiferal $\delta^{13}C$ and accumulation rates of organic carbon: *Uvigerina peregrina* group and *Cibicidoides wuellerstorfi*. Paleoceanography 1, 27–42.

Manuscript received October 12, 1999
Revision accepted December 16, 1999